

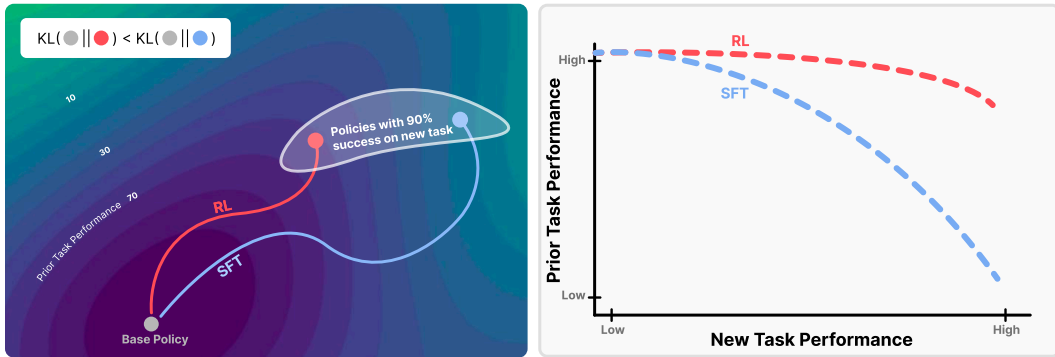
# 000 RL'S RAZOR: WHY ONLINE REINFORCEMENT 001 LEARNING FORGETS LESS 002

003 **Anonymous authors**

004 Paper under double-blind review

## 005 ABSTRACT

006  
007  
008  
009  
010  
011 Comparison of fine-tuning models with reinforcement learning (RL) and super-  
012 viewed fine-tuning (SFT) reveals that, despite similar performance at a new task,  
013 RL preserves prior knowledge and capabilities significantly better. We find that  
014 the degree of forgetting is determined by the distributional shift, measured as the  
015 KL-divergence between the fine-tuned and base policy evaluated on the new task.  
016 Our analysis reveals that on-policy RL is implicitly biased towards KL-minimal  
017 solutions among the many that solve the new task, whereas SFT can converge  
018 to distributions arbitrarily far from the base model. We validate these findings  
019 through experiments with large language models and robotic foundation models  
020 and further provide theoretical justification for why on-policy RL updates lead to  
021 a smaller KL change. We term this principle *RL's Razor*: among all ways to solve  
022 a new task, RL prefers those closest in KL to the original model.



035  
036 **Figure 1: Bias toward KL-minimal solutions reduces forgetting.** *Left:* Among policies that solve  
037 the new task, RL converges to those closest in KL to the base model. *Right:* This KL bias yields  
038 higher prior-task retention at matched new-task performance compared to SFT.

## 040 1 INTRODUCTION

043 Foundation models have rapidly become the backbone of modern AI, powering applications in  
044 language, vision, robotics, and beyond. Despite their remarkable capabilities, today's models are  
045 largely *static* once deployed: they excel at tasks learned during pre-training or post-training, but are  
046 not designed to self-improve and continually acquire new capabilities. We imagine a future where  
047 deployed models are long-lived *agents* assisting humans in the long-term and continuously adapting  
048 to new needs. As such, models must improve and adapt to new data, environments, and objectives  
049 Gao et al. (2025); Dao & Le (2025); Moradi et al. (2025); Li et al. (2025b); Simonds & Yoshiyama  
050 (2025); Zweiger et al. (2025).

051 A central challenge to this vision is *catastrophic forgetting*—the tendency for models to lose previ-  
052 ously acquired capabilities when trained on new tasks McCloskey & Cohen (1989); French (1999);  
053 Kirkpatrick et al. (2017); Luo et al. (2023). Although scaling model size and pre-training data  
improves robustness Ramasesh et al. (2021); Luo et al. (2023); Cossu et al. (2024), catastrophic

forgetting remains a persistent obstacle, undermining the promise of continual improvement Bommasani (2021); Guo et al. (2025b); Zweiger et al. (2025). To enable foundation models to serve as long-term agents, we need to develop post-training methods that allow models to acquire new skills without erasing old ones.

To further this goal, we analyze the performance of two widely used post-training schemes of supervised fine-tuning (SFT) and reinforcement learning (RL). Our experiments reveal a surprising finding: even when SFT and RL achieve the same performance on the new task, we observe that **SFT often achieves new-task gains by erasing prior knowledge, while RL better preserves old skills**. Figure 1 (right) illustrates this tradeoff: although both methods can reach high performance on the new task, RL maintains substantially higher performance on prior tasks compared to SFT.

This striking empirical gap raises the question: what underlying mechanism allows RL to improve on new tasks, but unlike SFT, minimally impacts the model’s prior knowledge?

Previous approaches to catastrophic forgetting targeted specific factors such as constraining weight updates (Kirkpatrick et al., 2017; Aljundi et al., 2018; Zenke et al., 2017), preserving learned features (Rannen et al., 2017; Hou et al., 2019), or regularizing shift in output distribution (Li & Hoiem, 2017; Stiennon et al., 2020). While these methods can reduce forgetting, they focus on its effects rather than its underlying cause. Consequently, it remains unclear what truly governs forgetting or why different training algorithms behave so differently. Some prior work claimed that forgetting can be determined by how much the model’s distribution shifts on past tasks (Rebuffi et al., 2017; Castro et al., 2018; Chaudhry et al., 2018; Wu et al., 2019). Yet in practice, this is infeasible to measure in foundation models, where the set of prior tasks is vast or even unbounded. To search for a more useful principle, we systematically ablated many candidate variables. Surprisingly, we find that forgetting can instead be predicted using only the *new* task distribution. Specifically, we uncover an **empirical forgetting law: When fine-tuning a model  $\pi$  on a new task  $\tau$ , the degree of forgetting is accurately predicted by  $\mathbb{E}_{x \sim \tau} [\text{KL}(\pi_0 || \pi)]$** , the KL divergence between the fine-tuned and base policy evaluated on the new task. This law is practically useful since it can be measured, and even influenced, during fine-tuning, without requiring access to past-task data. Although the mechanism remains to be fully understood, the consistency of this law across models and domains suggests it reflects a fundamental property of forgetting.

This law also clarifies the surprising difference between SFT and RL. Our analysis reveals a simple but powerful principle we call **RL’s Razor: among the many high-reward solutions for a new task, on-policy methods such as RL are inherently biased toward solutions that remain closer to the original policy in KL divergence**. Figure 1 (left) highlights this effect: among the many policies that reach a high success rate on the new task, RL is biased toward KL-minimal solutions, while SFT can converge to distant ones. This bias arises directly from RL’s *on-policy training*: by sampling from the model’s own distribution at every step, RL constrains learning to outputs already given non-negligible probability by the base model. To improve reward, these samples are reweighted and used to update the model, which gradually shifts the policy rather than pulling it toward an arbitrary distribution. Thus, when multiple equally good solutions exist for a new task, RL tends to find solutions close to the original policy, while SFT can converge to solutions much farther away, depending on the provided labels. Theoretical analysis in a simplified setting confirms this view, showing that policy gradient methods converge to KL-minimal solutions even without explicit regularization.

Finally, to validate the KL hypothesis, we construct an “oracle SFT” distribution that provably minimizes KL divergence while achieving perfect accuracy. Training on this oracle distribution produces even less forgetting than RL itself. This demonstrates that RL’s advantage does not stem from being inherently different, but from its implicit KL minimization. Whenever training is biased toward KL-minimal solutions, forgetting is reduced.

Our main contributions are:

- We show that RL fine-tuning forgets less than SFT, even when both reach the same performance on new tasks.
- We uncover an empirical forgetting law: the KL divergence to the base policy, measured on the new task, as a strong predictor of catastrophic forgetting across objectives and hyperparameters.

108 • We provide empirical and theoretical evidence that the on-policy nature of policy gradient methods  
 109 leads to smaller KL shifts and explains RL’s advantage.  
 110

111 Together, these findings suggest a new perspective on post-training: to achieve continual adapta-  
 112 tion without forgetting, algorithms should explicitly aim to minimize KL divergence from the base  
 113 model. This principle opens the door to designing future training methods that combine RL’s ability  
 114 to preserve prior knowledge with the efficiency of SFT, enabling foundation models that can truly  
 115 *learn for life*.

116  
 117 **2 RELATED WORK**  
 118

119 **Foundation Models and Post-training** In modern deep learning, large-scale models pre-trained  
 120 on broad, diverse datasets (usually termed Foundation models) serve as general-purpose back-  
 121 bones (Radford et al., 2021; Achiam et al., 2023; Touvron et al., 2023; Hu et al., 2023; Li et al.,  
 122 2024a) with broad domain knowledge and some zero-shot learning abilities (Radford et al., 2018;  
 123 Brown et al., 2020). However, pre-trained models may not directly meet the requirements of specific  
 124 applications or align with domain-specific constraints. Post-training methods address this gap by  
 125 adapting foundation models to downstream tasks through supervised fine-tuning on curated datasets  
 126 (Howard & Ruder, 2018; Dodge et al., 2020; Wei et al., 2021; Chung et al., 2024), reinforcement  
 127 learning from human or automated feedback (Ziegler et al., 2019; Ouyang et al., 2022; Guo et al.,  
 128 2025a; Zhai et al., 2024), and other techniques (Rafailov et al., 2023). In this work, we study how  
 129 different post-training methods affect forgetting, focusing on supervised fine-tuning and reinforce-  
 130 ment learning.

131 **Catastrophic Forgetting.** While fine-tuning primarily aims to improve performance on a new  
 132 specific task, preserving the model’s pre-existing general capabilities is equally critical. Unfortu-  
 133 nately, fine-tuning often leads to catastrophic forgetting—a phenomenon where learning new in-  
 134 formation significantly deteriorates previously acquired knowledge McCloskey & Cohen (1989);  
 135 French (1999); Kirkpatrick et al. (2017); Ouyang et al. (2022); Luo et al. (2023). Many works have  
 136 sought to reduce forgetting by constraining updates, for example, by penalizing the magnitude of  
 137 change in the model parameters, features, or matching the output on previous tasks/datasets (Wang  
 138 et al., 2024). These methods are effective heuristics, but they address the symptoms of forgetting  
 139 rather than explaining its cause. Our aim is to identify a simple and predictive metric that explains  
 140 when and why forgetting occurs across different training algorithms.

141 We do not introduce a new training algorithm, but instead identify a simple *empirical forgetting*  
 142 law: the KL divergence between the fine-tuned and base policy, measured *on the new task*, reliably  
 143 predicts the degree of forgetting. The law also sheds light on why some mitigation strategies work.  
 144 For example, methods like Elastic Weight Consolidation (Kirkpatrick et al., 2017) can be seen as  
 145 approximations to KL minimization (Chaudhry et al., 2018). Interestingly, practitioners have also  
 146 observed that KL regularization used in RL fine-tuning of LLMs as a heuristic for stabilizing opti-  
 147 mization or preventing reward hacking Stiennon et al. (2020); Gao et al. (2023), also helps reduce  
 148 catastrophic forgetting (Ouyang et al., 2022). Our contribution is to show that KL divergence is not  
 149 merely a useful heuristic, but a reliable predictor of forgetting across settings.

150 **SFT versus RL.** Prior comparisons between SFT and RL have focused on new task performance.  
 151 A seminal result in sequential decision making is that on-policy learning can achieve stronger per-  
 152 formance even when the expert providing supervision is the same one used to generate the offline  
 153 dataset (Ross et al., 2011). Recent empirical studies have also found that RL fine-tuned models often  
 154 exhibit superior generalization beyond the training distribution Han et al. (2025); Chu et al. (2025);  
 155 Li et al. (2025a) and transfer more effectively to related tasks Huan et al. (2025) compared to SFT.  
 156 However, prior works haven’t examined the relative susceptibility of RL and SFT to catastrophic  
 157 forgetting, which is the focus of our study.

158 Concurrently, Lai et al. (2025) reports that RL forgets less than SFT, but ascribes RL’s advantage  
 159 to learning from negative examples and not to the on-policy nature of RL. Results in Section 5  
 160 contradict their explanation of why RL forgets less, showing that the on-policy nature of RL is key.  
 161 We also contribute the empirical forgetting law, the RL Razor, and its theoretical justification.

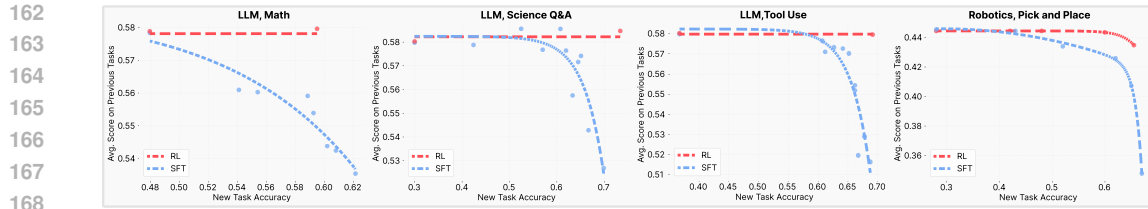


Figure 2: **Pareto frontiers of RL and SFT.** Comparing the performance of a fine-tuned model on the new task (x-axis) and prior task (y-axis). Each point corresponds to a model trained with a different set of hyperparameters, and the curves trace the Pareto frontiers for the two methods. RL achieves new-task improvements while maintaining prior knowledge, whereas SFT improves new-task performance at the expense of forgetting the prior task.

### 3 REINFORCEMENT LEARNING FORGETS LESS THAN SFT

We report results comparing the degree of catastrophic forgetting against new-task performance induced by RL and SFT on various large language model (LLM) and simulated robotic tasks.

#### 3.1 PERFORMANCE TRADE-OFFS

**Experimental Setup.** For each new task, we fine-tuned models using the same set of prompts. One group of models was trained with SFT, and another with RL using GRPO Shao et al. (2024). In RL training, we used only a binary success indicator as the reward, *without explicit KL regularization*. Evaluation was performed along two axes:

- New task Performance: We measured performance on the held-out test set of the newly introduced task to assess the performance gain from the training.
- Previous tasks Performance: We measured performance on a diverse set of unrelated benchmarks. A drop in these benchmarks was taken as a measure of catastrophic forgetting.

Since different hyperparameters can lead to varying trade-offs between learning and forgetting, we trained dozens of models under diverse hyperparameter settings for both SFT and RL. To compare methods fairly, we identify the Pareto frontier in the two-dimensional plane of new-task performance versus previous-task performance. The Pareto frontier represents the set of models for which no further improvement on the new task is possible without incurring greater forgetting. Figure 2 (right) reports these frontiers: each point corresponds to a trained model with a different set of hyperparameters, and the Pareto-frontier curve indicates the best achievable trade-off for each method.

**Tasks and Datasets.** We perform experiments across three LLM and a single robotic tasks:

- *LLM, Math reasoning*: Qwen 2.5 3B-Instruct (Qwen et al., 2025) trained on math questions from the Open-Reasoner-Zero dataset (Hu et al., 2025).
- *LLM, Science Q&A*: Qwen 2.5 3B-Instruct trained on Chemistry L-3 subset of SciKnowEval (Feng et al., 2024).
- *LLM, Tool use*: Qwen 2.5 3B-Instruct trained on ToolAlpaca dataset (Tang et al., 2023).
- *Robotics, Pick and Place*: OpenVLA 7B (Kim et al., 2024) trained in the SimplerEnv environment (Li et al., 2024b) on the task of picking up a can.

To measure forgetting, we evaluated the finetuned models on established benchmarks covering diverse prior capabilities. For LLMs, we used Hellaswag (Zellers et al., 2019), TruthfulQA (Lin et al., 2021), MMLU (Hendrycks et al., 2020), IFEval (Zhou et al., 2023), Winogrande (Sakaguchi et al., 2021), and HumanEval (Chen et al., 2021). For robotic policies, we evaluated on the open/close drawer SimplerEnv tasks, excluding the one used for fine-tuning. These benchmarks act as proxies for prior skills that should be preserved during adaptation. Full details on SFT data sources, hyperparameters, and training/evaluation protocols are provided in Appendix C.

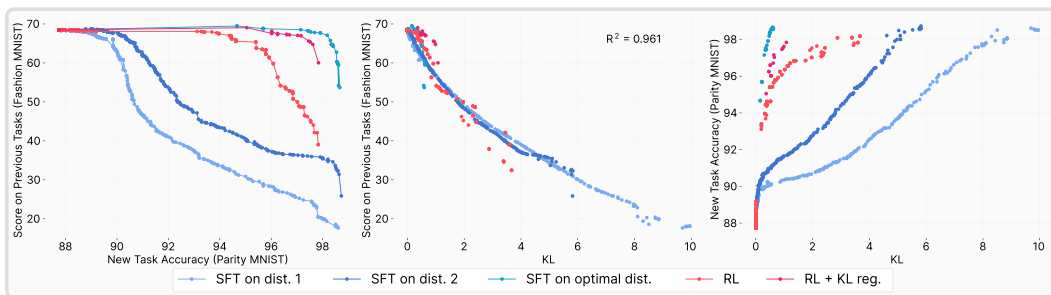


Figure 3: **KL divergence predicts catastrophic forgetting.** (Left) Learning-Forgetting Trade-offs. SFT outperform RL only when an oracle distribution is used as a source of annotation. (Middle) Forgetting aligns to a single curve when plotted against KL divergence, showing KL as a strong predictor across methods. (Right) RL improves new-task accuracy with much smaller KL shifts than SFT, highlighting the conservativeness of on-policy updates.

**Results.** Figure 2 reports the trade-off between new-task performance and retention of prior abilities. For RL, as accuracy on the new task increases, performance on previous benchmarks remains nearly unchanged. In contrast, SFT improvements on the new task consistently come at the cost of substantial forgetting. This difference is most pronounced in *Math*, where even small gains on the fine-tuned task correspond to a sharp reduction in prior-task performance. In *Science Q&A* and *Tool Use*, SFT retains some ability on prior tasks at lower accuracy levels for the new task, but performance deteriorates rapidly as the model approaches higher accuracy on the new task.

#### Takeaway 1

RL is able to learn new tasks while incurring minimal forgetting, whereas SFT reaches similar new-task performance only by sacrificing prior knowledge.

## 4 SMALLER KL DIVERGENCES LEAD TO LESS FORGETTING

As shown in Section 3, RL fine-tuning achieves comparable new-task performance to SFT while consistently forgetting less. Explaining this gap requires identifying a variable that determines the degree of forgetting across methods. We therefore searched for a predictor that could account for forgetting independently of the training algorithm or hyperparameters. Such a predictor would both explain the empirical difference between RL and SFT and offer a unifying principle for catastrophic forgetting. Prior work has proposed candidates such as the magnitude of weight changes, sparsity of updates, or gradient rank. Across our experiments, however, none of these variables consistently aligned with the observed forgetting behavior (see Section 6). What did emerge was an *empirical forgetting law*: the **KL divergence between the fine-tuned model and the base model, measured on the new task**, reliably predicts the degree of forgetting.

Testing this hypothesis in large LLMs is challenging, since RL training is computationally expensive and cannot easily be run to convergence. Moreover, the search for predictors requires repeating fine-tuning many times under diverse conditions. To address these limitations, we designed a controlled toy setting, ParityMNIST, that allows us to replicate the RL-SFT gap under full convergence and perform systematic ablations.

ParityMNIST is derived from MNIST (Deng, 2012), but reframes the task as predicting parity (even vs. odd). An image of an even digit is correctly classified if the model predicts *any* even digit label, and likewise for odd digits. Multiple output distributions are thus equally valid, mirroring a key property of the generative tasks we studied in section 3: *many distinct policies can achieve the same performance*.

We pretrained a 3-layer MLP jointly on a subset of ParityMNIST and FashionMNIST (Xiao et al., 2017), then fine-tuned only on ParityMNIST while measuring forgetting on FashionMNIST. This

270 design provides a minimal, tractable setting for investigating predictors of forgetting. To parallel the  
 271 main experiments:

273 • In the **SFT** setting, the model was trained on labels sampled from a single arbitrary distribution  
 274 out of the many possible correct ones.

275 • In the **RL** setting, the reward was correctness with respect to parity, leaving the model free to  
 276 converge to any valid distribution.

278 For more details, see Appendix C.3. This design allowed us to replicate the phenomenon where RL  
 279 reached high accuracy on the new task with substantially slower degradation of prior knowledge,  
 280 while SFT exhibited a steeper trade-off (Figure 3, left). Importantly, *reproducing the effect in this*  
 281 *simple MLP setting shows that it is not specific to large scale transformers, but a more general*  
 282 *property of fine-tuning deep generative models.*

283 **KL as Predictor.** Plotting forgetting against the KL divergence from the base model on ParityMNIST  
 284 reveals a single functional relationship across both RL and SFT (Figure 3, middle). This  
 285 indicates that forgetting is determined by KL divergence, not by the choice of training algorithm. A  
 286 quadratic fit achieves  $R^2 = 0.96$  in this setting, underscoring the strength of the relationship. To test  
 287 robustness, we repeated the experiment with two different arbitrary SFT labelings. Although their  
 288 Pareto frontiers differed, the forgetting–KL curves coincided, confirming that KL consistently pre-  
 289 dicted forgetting irrespective of training method or label distribution. The same correlation appears  
 290 in our LLM experiments, with a quadratic fit achieving  $R^2 = 0.71$  (Figure 12). While weaker, the  
 291 residuals are mean-zero and can be attributed to noise from approximate KL and accuracy estima-  
 292 tion.

293 **Optimal SFT Distribution.** To validate that KL divergence is the predictor variable, we con-  
 294 structed an oracle SFT distribution. In ParityMNIST, the simplicity of the task allows us to analyt-  
 295 ically identify the labeling that minimizes KL divergence to the base model among all distributions  
 296 achieving 100% accuracy (Appendix C.3). If KL divergence fully determines forgetting, then train-  
 297 ing SFT on this oracle distribution should yield the optimal accuracy–forgetting trade-off. The  
 298 results in Figure 3 confirm this prediction—SFT trained on the oracle distribution retained more  
 299 prior knowledge than RL, achieving the best trade-off observed. RL performs well because its on-  
 300 policy updates bias the solution toward low-KL regions, but when SFT is explicitly guided to the  
 301 KL-minimal distribution, it can surpass RL. As an additional validation, we trained an SFT model  
 302 on data generated by an RL-trained model. The distilled SFT matched RL’s accuracy–forgetting  
 303 trade-off (Figure 10), reinforcing that the distribution learned, rather than the optimization algo-  
 304 rithm, governs forgetting. Finally, we also added KL regularization to SFT, and found that it only  
 305 minimally improves the forgetting-learning Pareto frontier (Appendix A).

306 Takeaway 2

308 Catastrophic forgetting in both SFT and RL is predicted by the KL divergence between the  
 309 fine-tuned and base models on the new task.

312 

## 5 ON-POLICY METHODS LEADS TO SMALLER KL DIVERGENCE

315 Having established that the KL divergence between the trained model and its base distribution on  
 316 the new task predicts catastrophic forgetting, we now ask: why are RL fine-tuned models able to  
 317 achieve strong task performance while moving less in KL than SFT models?

318 

### 5.1 EXPERIMENTAL EVIDENCE

320 To understand the difference in KL behavior, it is useful to contrast the training objectives of SFT  
 321 and RL. For discrete outputs, SFT minimizes cross-entropy against a supervision distribution  $\pi_\beta$   
 322 over a distribution of inputs  $\mathcal{D}$ :

$$323 \mathcal{L}_{\text{SFT}}(\pi) = -\mathbb{E}_{x \sim \mathcal{D}, y \sim \pi_\beta} [\log \pi(y|x)]$$



Figure 4: **Comparison of algorithm classes.** (Left) The four quadrants illustrate algorithm types, defined by whether they are on-policy or offline and whether they incorporate negative gradients. (Middle) On-policy methods retain prior knowledge more effectively. (Right) Both GRPO and 1-0 Reinforce achieve higher new-task accuracy while incurring smaller KL shifts from the base model, showing that on-policy methods consistently induce more conservative KL updates.

In contrast, RL with policy gradients optimizes\*:

$$\mathcal{L}_{\text{RL}}(\pi) = -\mathbb{E}_{x \sim \mathcal{D}, y \sim \pi} [A(x, y) \log \pi(y|x)]$$

where  $A(x, y)$  is an Advantage function, which is the reward of  $y$  normalized with respect to other rewards for the same  $x$ . Two features distinguish this from SFT:

1. **Sampling Distribution.** While in RL the training was done on outputs drawn from the model’s own distribution, in SFT they come from fixed external annotations.
2. **Negative Examples.** While sampling from  $\pi$ , some of the responses will be incorrect. These are usually assigned a negative coefficient  $A(x, y)$ . This pushes probability mass away from poor outputs, a mechanism absent in SFT.

Our hypothesis is that one of these two differences is what causes RL’s resistance to forgetting. To examine our hypothesis, we perform experiments with four different objectives:

- **GRPO.** An on-policy objective that utilizes negative examples. Here,  $A(x, y)$  is the normalized reward.
- **1-0 Reinforce.** An on-policy algorithm that does not use negative examples. Here,  $A(x, y) = 1$  for correct responses and 0 for incorrect ones. This is equivalent to sampling from the model and performing SFT on correct answers only.
- **SFT.** An offline objective that does not use negative examples.
- **SimPO.** An offline objective that utilizes negative examples. We create negative examples by sampling incorrect responses from an external model, and use the SFT data for positive examples. The SimPO (Meng et al., 2024) loss compares correct and incorrect outputs via a logistic term:

$$\mathcal{L}_{\text{SimPO}}(\pi) = -\mathbb{E}_{x \sim \mathcal{D}, y_w \sim \pi_{\beta+}, y_l \sim \pi_{\beta-}} [\log \sigma (\log \pi(y_w|x) - \log \pi(y_l|x) - 1)]$$

where  $\pi_{\beta+}$  and  $\pi_{\beta-}$  denote distributions for correct and incorrect responses, respectively. We used SimPO rather than naïve likelihood/negative likelihood because the latter was unstable to train.

We compared the four objectives on the Science Q&A task, measuring their learning-forgetting trade-offs as in Section 4. The results, shown in Figure 4, reveal that 1-0 Reinforce behaves similarly to GRPO, while SimPO resembles SFT. Thus, the critical factor is not the presence of negative gradients but the use of on-policy data. Plotting KL divergence confirms this conclusion: on-policy methods (GRPO and 1-0 Reinforce) reach the same task performance with significantly smaller KL divergence from the base model than offline methods (SFT and SimPO).

## 5.2 THEORETICAL PERSPECTIVE

\*Notice that in practice, the policy gradient trick (Sutton et al., 1998) ensures gradients are taken only through the log-probability term, not through the sampling distribution inside the expectation.

378 Beyond the empirical results, it is useful to ask why on-  
 379 policy methods naturally induce smaller KL shifts. One  
 380 way to see this is through the lens of projection in prob-  
 381 ability space: policy gradient methods can be understood  
 382 as a conservative projection that keeps the policy close to  
 383 its starting point while reweighting toward higher-reward  
 384 outcomes. At each step, the policy samples outputs it al-  
 385 ready finds likely, then re-weights those samples accord-  
 386 ing to reward, shifting probability mass toward higher-  
 387 reward outcomes while suppressing lower-reward ones.  
 388 Crucially, because updates are defined relative to the  
 389 model’s own distribution, they nudge the policy toward  
 390 a nearby re-weighted distribution, rather than pulling it  
 391 toward a potentially distant external distribution (as in  
 392 SFT). This explains why policy gradient methods tend to  
 393 remain close to the base model in KL divergence.

394 This perspective can be formalized by observing that, in the binary-reward case, the re-weighted  
 395 distribution targeted by policy gradient is exactly the minimum-KL projection of the current policy  
 396 onto the set of optimal ones.

397 **Lemma 5.1.** *Let  $p$  be a distribution over a finite set  $Y$ , and let  $R : Y \rightarrow \{0, 1\}$  be a reward  
 398 function. Rejection sampling from  $p$  with acceptance condition  $R(y) = 1$  yields a distribution  $q_{RS}$ .  
 399 This distribution can be equivalently characterized as the solution to:*

$$400 \quad q_{RS} = \arg \min_q D_{KL}(q || p) \quad s.t. \quad \mathbb{E}_{y \sim q}[R(y)] = 1$$

402 Building on this, we show that policy gradient converges to the KL-minimal optimal policy within  
 403 the representable family. A detailed version with proofs is provided in Appendix B.

404 **Theorem 5.2.** *Let  $Y$  be a finite set and let  $\Pi \subseteq \Delta(Y)$  be a convex family of feasible policies (e.g.,  
 405 an exponential family). Let  $R : Y \rightarrow \{0, 1\}$  be a binary reward function and  $P^* = \{q : \mathbb{E}_q[R] = 1\}$   
 406 the set of optimal policies. Then, under suitable regularity conditions, solving the reinforcement  
 407 learning objective with policy gradient converges to*

$$408 \quad \pi^\dagger = \arg \min_{\pi \in P^* \cap \Pi} D_{KL}(\pi || \pi_0),$$

410 where  $\pi_0$  is the initialization. In other words, policy gradient selects, among all optimal repre-  
 411 sentable policies, the one closest in KL-divergence to the starting policy.

### 413 Takeaway 3

414 On-policy training explains why RL maintains smaller KL divergence than SFT. Sampling  
 415 from the model’s own distribution keeps it close to the base model, while SFT pushes it  
 416 toward arbitrary external distributions.

## 418 6 ALTERNATIVE HYPOTHESIS

420 Science advances not only by identifying the right explanations, but also by eliminating incorrect  
 421 ones. To this end, we systematically evaluated alternative variables as potential predictors of catas-  
 422 troptic forgetting, grouped into four categories:

- 424 **• Weight-level changes.** Many prior work tried to mitigate forgetting by constraining the change  
 425 in parameter space (Kirkpatrick et al., 2017; Aljundi et al., 2018; Zenke et al., 2017). We mea-  
 426 sured parameter changes under  $L_1$ , Fisher-weighted  $L_2$ , and spectral norm metrics. The Fisher  
 427 matrix was computed on the basis of the model parameters, with expectation over inputs from the  
 428 previous task. These metrics correlated only weakly with forgetting: large parameter shifts could  
 429 occur without forgetting, and conversely, forgetting sometimes occurred despite small parameter  
 430 movement.
- **Representation-level changes.** Some other papers focused on maintaining the previous features  
 (Jung et al., 2018; Hou et al., 2019; Dhar et al., 2019). We examined hidden activation shifts

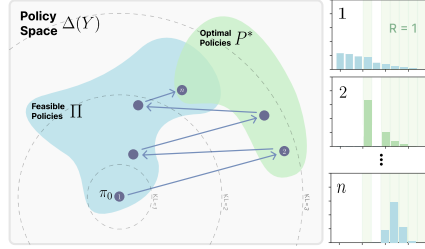


Figure 5: **KL-minimal path to optimality.** Alternating I-projection into the set of optimal policies and M-projection into  $\Pi$  carries  $\pi_0$  into  $P^*$  while preferring the closest solution in KL.

(L1 and L2 distances) as proxies for changes in internal representations. Although we found that there is representation drift during training (see Appendix D.1), the curves were distinct between training objectives, meaning that it is not a good predictor.

- **Sparsity and rank of updates.** Motivated by Mukherjee et al. (2025), who argue that RL updates are sparse while SFT weight updates are dense, we explicitly tested this hypothesis. We found that the reason for the observed sparsity was the use of `bfloat16` for model training. Since `bfloat16` has a limited mantissa, small parameter updates (such as those produced by RL) can fail to cross the representational threshold, effectively causing no update at all. Performing the same training with `float32` resulted in models with identical performance but without any sparsity in their weight updates. The rank of all weight updates was full.
- **Distributional distances.** We considered multiple measures of output distribution change, all measured over inputs from the new task  $\tau$ : Forward KL ( $\mathbb{E}_{x \sim \tau} [\text{KL}(\pi_0 || \pi)]$ ), Reverse KL ( $\mathbb{E}_{x \sim \tau} [\text{KL}(\pi || \pi_0)]$ ), Total Variation, and  $L_2$  distance between distributions.

Table 1 summarizes these results for the MNIST task. Across all candidates, KL divergence (both forward and reverse) between the fine-tuned and base model evaluated on the new task emerges as the only consistent and high-fidelity predictor of catastrophic forgetting.

Variable	$R^2$ (2nd deg. polynomial)
KL, forward	<b>0.96 ± 0.01</b>
KL, reverse	0.93 ± 0.01
TV	0.80 ± 0.01
Distribution change, $L_2$	0.56 ± 0.02
Weight change, L1	0.34 ± 0.02
Weight change, Fisher Weighted $L_2$	0.58 ± 0.02
Weight change, spectral norm	0.58 ± 0.02
Sparsity of weight change	N/A
Rank of weight change	N/A
Activation change, L1	0.52 ± 0.02
Activation change, $L_2$	0.55 ± 0.02

Table 1: Predictive power of alternative variables compared to KL.

## 7 DISCUSSION AND CONCLUSION

Our study reveals that catastrophic forgetting is governed not by the choice of training algorithm, but by the KL divergence from the base policy evaluated on the new task. This explains why RL forgets less than SFT, as on-policy training naturally biases updates toward KL-minimal solutions, preserving prior knowledge while acquiring new skills.

However, we still lack a mechanistic account of why larger KL shifts on the new task disrupt prior knowledge—whether through representational interference, implicit capacity limits, or other dynamics. Moreover, while we demonstrate the KL-forgetting link across moderate-scale LLMs and toy models, its behavior at frontier scales and in more diverse generative domains remains unknown. In addition, we didn’t study online but off-policy algorithms, which are popular in RL. Addressing these gaps will be essential for grounding the principle and extending it to real-world deployment.

Taken together, our results motivate a new design axis for post-training research: algorithms should be judged not only by how well they optimize new tasks, but also by how conservatively they move in KL relative to the base model. Importantly, this does not mean offline data cannot help, but that continual learning requires updates to keep learning close to the KL-minimal path. Embracing this principle may allow us to build agents that not only learn new skills, but also truly learn for life.

## 8 USE OF LANGUAGE MODELS

The authors used large language models to polish and revise the writing of the manuscript. The models were not used to generate ideas, perform analysis, or produce original scientific content.

486 REFERENCES  
487

488 Josh Achiam, Steven Adler, Sandhini Agarwal, Lama Ahmad, Ilge Akkaya, Florencia Leoni Ale-  
489 man, Diogo Almeida, Janko Altenschmidt, Sam Altman, Shyamal Anadkat, et al. Gpt-4 technical  
490 report. *arXiv preprint arXiv:2303.08774*, 2023.

491 Rahaf Aljundi, Francesca Babiloni, Mohamed Elhoseiny, Marcus Rohrbach, and Tinne Tuytelaars.  
492 Memory aware synapses: Learning what (not) to forget. In *Proceedings of the European confer-  
493 ence on computer vision (ECCV)*, pp. 139–154, 2018.

494 Shun-ichi Amari and Hiroshi Nagaoka. *Methods of information geometry*, volume 191. American  
495 Mathematical Soc., 2000.

496 Rishi Bommasani. On the opportunities and risks of foundation models. *arXiv preprint  
497 arXiv:2108.07258*, 2021.

498 Anthony Brohan, Noah Brown, Justice Carbajal, Yevgen Chebotar, Joseph Dabis, Chelsea Finn,  
499 Keerthana Gopalakrishnan, Karol Hausman, Alex Herzog, Jasmine Hsu, et al. Rt-1: Robotics  
500 transformer for real-world control at scale. *arXiv preprint arXiv:2212.06817*, 2022.

501 Tom Brown, Benjamin Mann, Nick Ryder, Melanie Subbiah, Jared D Kaplan, Prafulla Dhariwal,  
502 Arvind Neelakantan, Pranav Shyam, Girish Sastry, Amanda Askell, et al. Language models are  
503 few-shot learners. *Advances in neural information processing systems*, 33:1877–1901, 2020.

504 Francisco M Castro, Manuel J Marín-Jiménez, Nicolás Guil, Cordelia Schmid, and Karteek Alahari.  
505 End-to-end incremental learning. In *Proceedings of the European conference on computer vision  
(ECCV)*, pp. 233–248, 2018.

506 Arslan Chaudhry, Puneet K Dokania, Thalaiyasingam Ajanthan, and Philip HS Torr. Riemannian  
507 walk for incremental learning: Understanding forgetting and intransigence. In *Proceedings of the  
508 European conference on computer vision (ECCV)*, pp. 532–547, 2018.

509 Mark Chen, Jerry Tworek, Heewoo Jun, Qiming Yuan, Henrique Ponde De Oliveira Pinto, Jared  
510 Kaplan, Harri Edwards, Yuri Burda, Nicholas Joseph, Greg Brockman, et al. Evaluating large  
511 language models trained on code. *arXiv preprint arXiv:2107.03374*, 2021.

512 Tianzhe Chu, Yuexiang Zhai, Jihan Yang, Shengbang Tong, Saining Xie, Dale Schuurmans, Quoc V  
513 Le, Sergey Levine, and Yi Ma. Sft memorizes, rl generalizes: A comparative study of foundation  
514 model post-training. *arXiv preprint arXiv:2501.17161*, 2025.

515 Hyung Won Chung, Le Hou, Shayne Longpre, Barret Zoph, Yi Tay, William Fedus, Yunxuan Li,  
516 Xuezhi Wang, Mostafa Dehghani, Siddhartha Brahma, et al. Scaling instruction-finetuned lan-  
517 guage models. *Journal of Machine Learning Research*, 25(70):1–53, 2024.

518 Andrea Cossu, Antonio Carta, Lucia Passaro, Vincenzo Lomonaco, Tinne Tuytelaars, and Davide  
519 Bacciu. Continual pre-training mitigates forgetting in language and vision. *Neural Networks*,  
520 179:106492, 2024.

521 Imre Csiszár. Information geometry and alternating minimization procedures. *Statistics and Deci-  
522 sions, Dedewicz*, 1:205–237, 1984.

523 Alan Dao and Thinh Le. Rezero: Enhancing llm search ability by trying one-more-time. *arXiv  
524 preprint arXiv:2504.11001*, 2025.

525 Arthur P Dempster, Nan M Laird, and Donald B Rubin. Maximum likelihood from incomplete data  
526 via the em algorithm. *Journal of the royal statistical society: series B (methodological)*, 39(1):  
527 1–22, 1977.

528 Li Deng. The mnist database of handwritten digit images for machine learning research [best of the  
529 web]. *IEEE signal processing magazine*, 29(6):141–142, 2012.

530 Prithviraj Dhar, Rajat Vikram Singh, Kuan-Chuan Peng, Ziyan Wu, and Rama Chellappa. Learning  
531 without memorizing. In *Proceedings of the IEEE/CVF conference on computer vision and pattern  
532 recognition*, pp. 5138–5146, 2019.

540 Jesse Dodge, Gabriel Ilharco, Roy Schwartz, Ali Farhadi, Hannaneh Hajishirzi, and Noah Smith.  
 541 Fine-tuning pretrained language models: Weight initializations, data orders, and early stopping.  
 542 *arXiv preprint arXiv:2002.06305*, 2020.

543 Kehua Feng, Keyan Ding, Weijie Wang, Xiang Zhuang, Zeyuan Wang, Ming Qin, Yu Zhao, Jianhua  
 544 Yao, Qiang Zhang, and Huajun Chen. Sciknoweval: Evaluating multi-level scientific knowledge  
 545 of large language models. *arXiv preprint arXiv:2406.09098*, 2024.

546 Robert M French. Catastrophic forgetting in connectionist networks. *Trends in cognitive sciences*,  
 547 3(4):128–135, 1999.

548 Huan-ang Gao, Jiayi Geng, Wenyue Hua, Mengkang Hu, Xinzhe Juan, Hongzhang Liu, Shilong  
 549 Liu, Jiahao Qiu, Xuan Qi, Yiran Wu, et al. A survey of self-evolving agents: On path to artificial  
 550 super intelligence. *arXiv preprint arXiv:2507.21046*, 2025.

551 Leo Gao, John Schulman, and Jacob Hilton. Scaling laws for reward model overoptimization. In  
 552 *International Conference on Machine Learning*, pp. 10835–10866. PMLR, 2023.

553 Leo Gao, Jonathan Tow, Baber Abbasi, Stella Biderman, Sid Black, Anthony DiPofi, Charles Fos-  
 554 ter, Laurence Golding, Jeffrey Hsu, Alain Le Noac'h, Haonan Li, Kyle McDonell, Niklas Muen-  
 555 nighoff, Chris Ociepa, Jason Phang, Laria Reynolds, Hailey Schoelkopf, Aviya Skowron, Lintang  
 556 Sutawika, Eric Tang, Anish Thite, Ben Wang, Kevin Wang, and Andy Zou. The language model  
 557 evaluation harness, 07 2024. URL <https://zenodo.org/records/12608602>.

558 Asela Gunawardana, William Byrne, and Michael I Jordan. Convergence theorems for generalized  
 559 alternating minimization procedures. *Journal of machine learning research*, 6(12), 2005.

560 Daya Guo, Dejian Yang, Haowei Zhang, Junxiao Song, Ruoyu Zhang, Runxin Xu, Qihao Zhu,  
 561 Shirong Ma, Peiyi Wang, Xiao Bi, et al. Deepseek-r1: Incentivizing reasoning capability in llms  
 562 via reinforcement learning. *arXiv preprint arXiv:2501.12948*, 2025a.

563 Haiyang Guo, Fanhu Zeng, Fei Zhu, Jiayi Wang, Xukai Wang, Jingang Zhou, Hongbo Zhao, Wen-  
 564 zhuo Liu, Shijie Ma, Da-Han Wang, et al. A comprehensive survey on continual learning in  
 565 generative models. *arXiv preprint arXiv:2506.13045*, 2025b.

566 Seungwook Han, Jyothish Pari, Samuel J Gershman, and Pulkit Agrawal. General reasoning requires  
 567 learning to reason from the get-go. *arXiv preprint arXiv:2502.19402*, 2025.

568 Dan Hendrycks, Collin Burns, Steven Basart, Andy Zou, Mantas Mazeika, Dawn Song, and  
 569 Jacob Steinhardt. Measuring massive multitask language understanding. *arXiv preprint  
 570 arXiv:2009.03300*, 2020.

571 Saihui Hou, Xinyu Pan, Chen Change Loy, Zilei Wang, and Dahua Lin. Learning a unified classifier  
 572 incrementally via rebalancing. In *Proceedings of the IEEE/CVF conference on computer vision  
 573 and pattern recognition*, pp. 831–839, 2019.

574 Jeremy Howard and Sebastian Ruder. Universal language model fine-tuning for text classification.  
 575 *arXiv preprint arXiv:1801.06146*, 2018.

576 Jingcheng Hu, Yinmin Zhang, Qi Han, Dixin Jiang, Xiangyu Zhang, and Heung-Yeung Shum.  
 577 Open-reasoner-zero: An open source approach to scaling up reinforcement learning on the base  
 578 model. *arXiv preprint arXiv:2503.24290*, 2025.

579 Yafei Hu, Quanting Xie, Vidhi Jain, Jonathan Francis, Jay Patrikar, Nikhil Keetha, Seungchan Kim,  
 580 Yaqi Xie, Tianyi Zhang, Hao-Shu Fang, et al. Toward general-purpose robots via foundation  
 581 models: A survey and meta-analysis. *arXiv preprint arXiv:2312.08782*, 2023.

582 Maggie Huan, Yuetai Li, Tuney Zheng, Xiaoyu Xu, Seungone Kim, Minxin Du, Radha Pooven-  
 583 dran, Graham Neubig, and Xiang Yue. Does math reasoning improve general llm capabilities?  
 584 understanding transferability of llm reasoning. *arXiv preprint arXiv:2507.00432*, 2025.

585 Minyoung Huh, Brian Cheung, Tongzhou Wang, and Phillip Isola. The platonic representation  
 586 hypothesis. *arXiv preprint arXiv:2405.07987*, 2024.

594 Heechul Jung, Jeongwoo Ju, Minju Jung, and Junmo Kim. Less-forgetful learning for domain ex-  
 595 pansion in deep neural networks. In *Proceedings of the AAAI conference on artificial intelligence*,  
 596 volume 32, 2018.

597

598 Moo Jin Kim, Karl Pertsch, Siddharth Karamcheti, Ted Xiao, Ashwin Balakrishna, Suraj Nair,  
 599 Rafael Rafailov, Ethan Foster, Grace Lam, Pannag Sanketi, et al. Openvla: An open-source  
 600 vision-language-action model. *arXiv preprint arXiv:2406.09246*, 2024.

601

602 James Kirkpatrick, Razvan Pascanu, Neil Rabinowitz, Joel Veness, Guillaume Desjardins, Andrei A  
 603 Rusu, Kieran Milan, John Quan, Tiago Ramalho, Agnieszka Grabska-Barwinska, et al. Overcom-  
 604 ing catastrophic forgetting in neural networks. *Proceedings of the national academy of sciences*,  
 605 114(13):3521–3526, 2017.

606

607 Tomasz Korbak, Ethan Perez, and Christopher L Buckley. RI with kl penalties is better viewed as  
 608 bayesian inference. *arXiv preprint arXiv:2205.11275*, 2022.

609

610 Simon Kornblith, Mohammad Norouzi, Honglak Lee, and Geoffrey Hinton. Similarity of neural  
 611 network representations revisited. In *International conference on machine learning*, pp. 3519–  
 3529. PMIR, 2019.

612

613 Song Lai, Haohan Zhao, Rong Feng, Changyi Ma, Wenzhuo Liu, Hongbo Zhao, Xi Lin, Dong  
 614 Yi, Min Xie, Qingfu Zhang, et al. Reinforcement fine-tuning naturally mitigates forgetting in  
 615 continual post-training. *arXiv preprint arXiv:2507.05386*, 2025.

616

617 Chunyuan Li, Zhe Gan, Zhengyuan Yang, Jianwei Yang, Linjie Li, Lijuan Wang, Jianfeng Gao, et al.  
 618 Multimodal foundation models: From specialists to general-purpose assistants. *Foundations and  
 Trends® in Computer Graphics and Vision*, 16(1-2):1–214, 2024a.

619

620 Tianle Li, Jihai Zhang, Yongming Rao, and Yu Cheng. Unveiling the compositional ability gap in  
 621 vision-language reasoning model. *arXiv preprint arXiv:2505.19406*, 2025a.

622

623 Xuanlin Li, Kyle Hsu, Jiayuan Gu, Karl Pertsch, Oier Mees, Homer Rich Walke, Chuyuan Fu,  
 624 Ishikaa Lunawat, Isabel Sieh, Sean Kirmani, Sergey Levine, Jiajun Wu, Chelsea Finn, Hao Su,  
 625 Quan Vuong, and Ted Xiao. Evaluating real-world robot manipulation policies in simulation.  
 626 *arXiv preprint arXiv:2405.05941*, 2024b.

627

628 Zhizhong Li and Derek Hoiem. Learning without forgetting. *IEEE transactions on pattern analysis  
 and machine intelligence*, 40(12):2935–2947, 2017.

629

630 Zhongyang Li, Ziyue Li, and Tianyi Zhou. C3po: Critical-layer, core-expert, collaborative pathway  
 631 optimization for test-time expert re-mixing. *ArXiv*, abs/2504.07964, 2025b. URL <https://api.semanticscholar.org/CorpusID:277667633>.

632

633 Stephanie Lin, Jacob Hilton, and Owain Evans. Truthfulqa: Measuring how models mimic human  
 634 falsehoods. *arXiv preprint arXiv:2109.07958*, 2021.

635

636 Zichen Liu, Changyu Chen, Wenjun Li, Penghui Qi, Tianyu Pang, Chao Du, Wee Sun Lee,  
 637 and Min Lin. Understanding r1-zero-like training: A critical perspective. *arXiv preprint  
 arXiv:2503.20783*, 2025.

638

639 Yun Luo, Zhen Yang, Fandong Meng, Yafu Li, Jie Zhou, and Yue Zhang. An empirical study  
 640 of catastrophic forgetting in large language models during continual fine-tuning. *arXiv preprint  
 arXiv:2308.08747*, 2023.

641

642 Michael McCloskey and Neal J Cohen. Catastrophic interference in connectionist networks: The  
 643 sequential learning problem. In *Psychology of learning and motivation*, volume 24, pp. 109–165.  
 644 Elsevier, 1989.

645

646 Yu Meng, Mengzhou Xia, and Danqi Chen. Simpo: Simple preference optimization with a  
 647 reference-free reward. *Advances in Neural Information Processing Systems*, 37:124198–124235,  
 2024.

648 Mohammad Mahdi Moradi, Hossam Amer, Sudhir Mudur, Weiwei Zhang, Yang Liu, and Walid  
 649 Ahmed. Continuous self-improvement of large language models by test-time training with  
 650 verifier-driven sample selection. *ArXiv*, abs/2505.19475, 2025. URL <https://api.semanticscholar.org/CorpusID:278905330>.

652 Sagnik Mukherjee, Lifan Yuan, Dilek Hakkani-Tur, and Hao Peng. Reinforcement learning finetunes  
 653 small subnetworks in large language models. *arXiv preprint arXiv:2505.11711*, 2025.

655 Long Ouyang, Jeffrey Wu, Xu Jiang, Diogo Almeida, Carroll Wainwright, Pamela Mishkin, Chong  
 656 Zhang, Sandhini Agarwal, Katarina Slama, Alex Ray, et al. Training language models to fol-  
 657 low instructions with human feedback. *Advances in neural information processing systems*, 35:  
 658 27730–27744, 2022.

659 Qwen, :, An Yang, Baosong Yang, Beichen Zhang, Binyuan Hui, Bo Zheng, Bowen Yu, Chengyuan  
 660 Li, Dayiheng Liu, Fei Huang, Haoran Wei, Huan Lin, Jian Yang, Jianhong Tu, Jianwei Zhang,  
 661 Jianxin Yang, Jiaxi Yang, Jingren Zhou, Junyang Lin, Kai Dang, Keming Lu, Keqin Bao, Kexin  
 662 Yang, Le Yu, Mei Li, Mingfeng Xue, Pei Zhang, Qin Zhu, Rui Men, Runji Lin, Tianhao Li,  
 663 Tianyi Tang, Tingyu Xia, Xingzhang Ren, Xuancheng Ren, Yang Fan, Yang Su, Yichang Zhang,  
 664 Yu Wan, Yuqiong Liu, Zeyu Cui, Zhenru Zhang, and Zihan Qiu. Qwen2.5 technical report, 2025.  
 665 URL <https://arxiv.org/abs/2412.15115>.

666 Alec Radford, Karthik Narasimhan, Tim Salimans, Ilya Sutskever, et al. Improving language under-  
 667 standing by generative pre-training. *arXiv preprint arXiv:2303.08774*, 2018.

668 Alec Radford, Jong Wook Kim, Chris Hallacy, Aditya Ramesh, Gabriel Goh, Sandhini Agarwal,  
 669 Girish Sastry, Amanda Askell, Pamela Mishkin, Jack Clark, et al. Learning transferable visual  
 670 models from natural language supervision. In *International conference on machine learning*, pp.  
 671 8748–8763. PMLR, 2021.

672 Rafael Rafailov, Archit Sharma, Eric Mitchell, Christopher D Manning, Stefano Ermon, and Chelsea  
 673 Finn. Direct preference optimization: Your language model is secretly a reward model. *Advances  
 674 in neural information processing systems*, 36:53728–53741, 2023.

675 Vinay Venkatesh Ramasesh, Aitor Lewkowycz, and Ethan Dyer. Effect of scale on catastrophic  
 676 forgetting in neural networks. In *International conference on learning representations*, 2021.

677 Amal Rannen, Rahaf Aljundi, Matthew B Blaschko, and Tinne Tuytelaars. Encoder based lifelong  
 678 learning. In *Proceedings of the IEEE international conference on computer vision*, pp. 1320–  
 679 1328, 2017.

680 Stéphane Ross, Geoffrey Gordon, and Drew Bagnell. A reduction of imitation learning and struc-  
 681 tured prediction to no-regret online learning. In *Proceedings of the fourteenth international con-  
 682 ference on artificial intelligence and statistics*, pp. 627–635. JMLR Workshop and Conference  
 683 Proceedings, 2011.

684 Keisuke Sakaguchi, Ronan Le Bras, Chandra Bhagavatula, and Yejin Choi. Winogrande: An adver-  
 685 sarial winograd schema challenge at scale. *Communications of the ACM*, 64(9):99–106, 2021.

686 Zhihong Shao, Peiyi Wang, Qihao Zhu, Runxin Xu, Junxiao Song, Xiao Bi, Haowei Zhang,  
 687 Mingchuan Zhang, YK Li, Yang Wu, et al. Deepseekmath: Pushing the limits of mathemati-  
 688 cal reasoning in open language models. *arXiv preprint arXiv:2402.03300*, 2024.

689 Toby Simonds and Akira Yoshiyama. Ladder: Self-improving llms through recursive problem de-  
 690 composition. *arXiv preprint arXiv:2503.00735*, 2025.

691 Nisan Stiennon, Long Ouyang, Jeffrey Wu, Daniel Ziegler, Ryan Lowe, Chelsea Voss, Alec Radford,  
 692 Dario Amodei, and Paul F Christiano. Learning to summarize with human feedback. *Advances  
 693 in neural information processing systems*, 33:3008–3021, 2020.

702 Richard S Sutton, Andrew G Barto, et al. *Reinforcement learning: An introduction*, volume 1. MIT  
 703 press Cambridge, 1998.  
 704

705 Qiaoyu Tang, Ziliang Deng, Hongyu Lin, Xianpei Han, Qiao Liang, Boxi Cao, and Le Sun. Toolal-  
 706 pac: Generalized tool learning for language models with 3000 simulated cases. *arXiv preprint*  
 707 *arXiv:2306.05301*, 2023.

708 Hugo Touvron, Thibaut Lavril, Gautier Izacard, Xavier Martinet, Marie-Anne Lachaux, Timothée  
 709 Lacroix, Baptiste Rozière, Naman Goyal, Eric Hambro, Faisal Azhar, et al. Llama: Open and  
 710 efficient foundation language models. *arXiv preprint arXiv:2302.13971*, 2023.

711 Nino Vieillard, Tadashi Kozuno, Bruno Scherrer, Olivier Pietquin, Rémi Munos, and Matthieu Geist.  
 712 Leverage the average: an analysis of kl regularization in reinforcement learning. *Advances in*  
 713 *Neural Information Processing Systems*, 33:12163–12174, 2020.

714

715 Liyuan Wang, Xingxing Zhang, Hang Su, and Jun Zhu. A comprehensive survey of continual  
 716 learning: Theory, method and application. *IEEE transactions on pattern analysis and machine*  
 717 *intelligence*, 46(8):5362–5383, 2024.

718 Jason Wei, Maarten Bosma, Vincent Y Zhao, Kelvin Guu, Adams Wei Yu, Brian Lester, Nan Du,  
 719 Andrew M Dai, and Quoc V Le. Finetuned language models are zero-shot learners. *arXiv preprint*  
 720 *arXiv:2109.01652*, 2021.

721

722 CF Jeff Wu. On the convergence properties of the em algorithm. *The Annals of statistics*, pp.  
 723 95–103, 1983.

724

725 Yue Wu, Yinpeng Chen, Lijuan Wang, Yuancheng Ye, Zicheng Liu, Yandong Guo, and Yun Fu.  
 726 Large scale incremental learning. In *Proceedings of the IEEE/CVF conference on computer vision*  
 727 *and pattern recognition*, pp. 374–382, 2019.

728 Han Xiao, Kashif Rasul, and Roland Vollgraf. Fashion-mnist: a novel image dataset for benchmark-  
 729 ing machine learning algorithms. *arXiv preprint arXiv:1708.07747*, 2017.

730

731 Rowan Zellers, Ari Holtzman, Yonatan Bisk, Ali Farhadi, and Yejin Choi. Hellaswag: Can a ma-  
 732 chine really finish your sentence? *arXiv preprint arXiv:1905.07830*, 2019.

733 Friedemann Zenke, Ben Poole, and Surya Ganguli. Continual learning through synaptic intelligence.  
 734 In *International conference on machine learning*, pp. 3987–3995. PMLR, 2017.

735

736 Simon Zhai, Hao Bai, Zipeng Lin, Jiayi Pan, Peter Tong, Yifei Zhou, Alane Suhr, Saining Xie, Yann  
 737 LeCun, Yi Ma, et al. Fine-tuning large vision-language models as decision-making agents via  
 738 reinforcement learning. *Advances in neural information processing systems*, 37:110935–110971,  
 739 2024.

740

741 Jeffrey Zhou, Tianjian Lu, Swaroop Mishra, Siddhartha Brahma, Sujoy Basu, Yi Luan, Denny  
 742 Zhou, and Le Hou. Instruction-following evaluation for large language models. *arXiv preprint*  
 743 *arXiv:2311.07911*, 2023.

744

745 Daniel M Ziegler, Nisan Stiennon, Jeffrey Wu, Tom B Brown, Alec Radford, Dario Amodei, Paul  
 746 Christiano, and Geoffrey Irving. Fine-tuning language models from human preferences. *arXiv*  
 747 *preprint arXiv:1909.08593*, 2019.

748

749 Adam Zweiger, Jyothish Pari, Han Guo, Ekin Akyürek, Yoon Kim, and Pulkit Agrawal.  
 750 Self-adapting language models. *ArXiv*, abs/2506.10943, 2025. URL <https://api.semanticscholar.org/CorpusID:279318966>.

751

752

753

754

755

756 A THE EFFECT OF KL REGULARIZATION  
757

758 In our main experiments, we did not employ explicit KL regularization. Nevertheless, our finding  
759 that forgetting is closely predicted by the KL divergence to the base model naturally raises the  
760 question: can directly regularizing KL divergence mitigate forgetting? This is especially relevant  
761 given that KL penalties are widely used in reinforcement learning fine-tuning of large language  
762 models (Stiennon et al., 2020; Ouyang et al., 2022; Vieillard et al., 2020).  
763

764 **Empirical observations.** We revisited the ParityMNIST setup from Section 4, this time adding explicit KL  
765 penalties to both SFT and RL training. For each method, we conducted a hyperparameter sweep and varied the  
766 regularization coefficient over 0.1, 0.2, 0.5. Figure A reports the resulting Pareto frontiers of the learning-forgetting  
767 trade-off. The effect is strikingly asymmetric:  
768

769 In RL, KL regularization substantially improves the  
770 trade-off. By explicitly discouraging large deviations  
771 from the base model, it amplifies RL’s inherent bias to-  
772 ward KL-minimal solutions, enabling gains on the new  
773 task while preserving performance on prior tasks.  
774

775 In SFT, KL regularization has only marginal effect. While  
776 it slightly restrains the model from drifting too far, the  
777 optimization remains tied to external supervision distributions,  
778 which may themselves be far from the KL-minimal  
779 solution. As a result, the overall frontier is essentially un-  
780 changed.  
781

782 These results suggest that explicit KL regularization cannot rescue SFT from its fundamental limitation:  
783 SFT is forced to imitate whatever distribution is provided, and cannot search for new solutions.  
784

785 **Theory** This intuition can be formalized. RL with KL regularization effectively restricts optimi-  
786 zation to policies achieving a given reward level and then selects the KL-minimal one. Thus,  
787 whenever the optimal reward is attainable, RL with a sufficiently small KL penalty converges to the  
788 minimum-KL optimal policy. By contrast, SFT with KL regularization minimizes cross-entropy to  
789 a fixed annotator distribution plus a KL penalty, and in general cannot guarantee alignment with the  
790 minimum-KL solution. Formally:

791 **Theorem A.1.** *Let  $\Delta$  be the set of probability measures on  $\mathcal{Y}$ , and  $\Pi \subseteq \Delta$  a nonempty feasible  
792 policy class. Fix a base policy  $\pi_0 \in \Pi$  and a reward  $R : \mathcal{Y} \rightarrow \mathbb{R}$ . let*  
793

$$R_{\max} = \sup_{\pi \in \Pi} \mathbb{E}_{\pi}[R], \quad P^* = \{\pi \in \Pi : \mathbb{E}_{\pi}[R] = R_{\max}\}$$

796 For  $\beta > 0$  consider the RL with KL regularization objective:  
797

$$\pi_{\beta}^{RL} = \arg \max_{\pi \in \Pi} \mathbb{E}_{\pi}[R] - \beta \text{KL}(\pi \| \pi_0)$$

800 if  $R_{\max}$  is attainable by the policy class then there exists  $\bar{\beta} > 0$  such that for all  $\beta \leq \bar{\beta}$ ,  
801

$$\pi_{\beta}^{RL} \in \arg \min_{\pi \in P^*} \text{KL}(\pi \| \pi_0)$$

804 Now, define annotator distribution  $q \in \Delta$ . For  $\beta > 0$ , consider the SFT with KL regularization  
805 objective:  
806

$$\pi_{\beta}^{SFT} = \arg \min_{\pi \in \Pi} -\mathbb{E}_{y \sim q} [\log \pi(y)] + \beta \text{KL}(\pi \| \pi_0)$$

807 In general, there is no  $\beta > 0$  for which  $\pi_{\beta}^{SFT}$  equals the minimum-KL optimal policy, even when  $q$   
808 itself is optimal ( $\mathbb{E}_q[R] = R_{\max}$ ).  
809

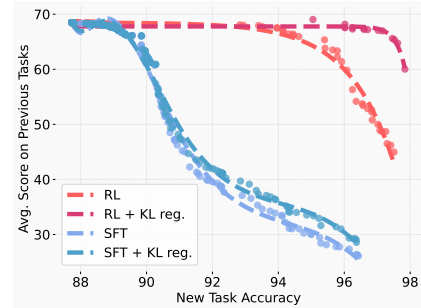


Figure 6: explicit KL regularization helps RL retain prior skills, but barely affects SFT training.

810 **B THEORY**  
811812 **B.1 IMPLICIT BIAS OF ON-POLICY RL**  
813

814 **Lemma B.1** (Rejection sampling as an I-projection). *Let  $p$  be a distribution over a finite set  $Y$ , and*  
 815 *let  $R : Y \rightarrow \{0, 1\}$  be a reward function. Rejection sampling from  $p$  with acceptance condition*  
 816  *$R(y) = 1$  yields a distribution  $q_{RS}$ . This distribution can be equivalently characterized as the*  
 817 *solution to:*

$$818 \quad q_{RS} = \arg \min_q D_{KL}(q || p) \quad s.t. \quad \mathbb{E}_{y \sim q}[R(y)] = 1$$

819 *Equivalently,  $q_{RS}$  is the I-projection of  $p$  onto the set  $\{q : \mathbb{E}_q[R] = 1\}$*

820 *Proof.* Let  $S = \{y \in Y : R(y) = 1\}$ . Rejection sampling produces the conditional distribution

$$823 \quad q_{RS}(y) = \begin{cases} \frac{p(y)}{p(S)} & y \in S, \\ 0 & y \notin S, \end{cases}$$

824 where  $p(S) = \sum_{y \in S} p(y)$  and we assume  $P(S) > 0$ .

825 Now consider the optimization problem. The constraint  $\mathbb{E}_q[R] = 1$  means

$$826 \quad \sum_{y \in Y} q(y)R(y) = \sum_{y \in S} q(y) = 1$$

827 so  $q$  must put all of its mass on  $S$ . Thus the feasible set is exactly all distributions supported on  $S$ .

828 For any  $q$  supported on  $S$ , we can write  $p(y) = p(S) p(y|S)$  for  $y \in S$ , and then

$$829 \quad \begin{aligned} D_{KL}(q || p) &= \sum_{y \in S} q(y) \log \frac{q(y)}{p(y)} = \sum_{y \in S} q(y) \log \frac{q(y)}{p(y|S)} - \log p(S) \sum_{y \in S} q(y) \\ 830 &= D_{KL}(q || p(\cdot | S)) - \log p(S) \end{aligned}$$

831 where we used  $\sum_{y \in S} q(y) = 1$  in the last step. The second term is constant in  $q$ , so minimizing  
 832  $D_{KL}(q || p)$  is the same as minimizing  $D_{KL}(q || p(\cdot | S))$ . By strict convexity of  $D_{KL}(\cdot || \cdot)$  in its first  
 833 argument, the unique minimizer is  $q = p(\cdot | S) = q_{RS}$ .  $\square$

834 **Lemma B.2** (Policy gradient as an M-projection). *Let  $Y$  be a finite set and let  $\Pi \subseteq \Delta(Y)$  be a*  
 835 *set of admissible policies (distributions over  $Y$ ). Consider the single-step reinforcement learning*  
 836 *objective*

$$837 \quad \max_{\pi} \mathbb{E}_{y \sim \pi}[R(y)]$$

838 where  $R : Y \rightarrow \mathbb{R}_{\geq 0}$  is a reward function. By the policy gradient theorem, this objective is equivalently optimized by

$$839 \quad \max_{\pi} \mathbb{E}_{y \sim \bar{\pi}}[R(y) \log \pi(y)]$$

840 where  $\bar{\pi}$  indicates that gradients are not propagated through the sampling distribution. Define the  
 841 distribution

$$842 \quad q(y) = \frac{\pi(y)R(y)}{Z}, \quad Z = \sum_{y \in Y} \pi(y)R(y)$$

843 Then taking a policy gradient step is equivalent to taking a gradient step on the following objective:

$$844 \quad \min_{\pi} -\mathbb{E}_{y \sim q}[\log \pi(y)]$$

845 In other words, optimizing the RL objective using policy gradient is equivalent to finding the M-  
 846 projection of  $q$  onto the set of feasible policies  $\pi$  using gradient descent.

847 *Proof.* Expanding the policy gradient objective gives

$$848 \quad \mathbb{E}_{y \sim \bar{\pi}}[R(y) \log \pi(y)] = \sum_{y \in Y} \pi(y)R(y) \log \pi(y)$$

864 Let  $Z = \sum_{y \in Y} \pi(y)R(y)$ . Define  $q(y) = \pi(y)R(y)/Z$ . Then the above becomes  
 865

$$866 \sum_{y \in Y} \pi(y)R(y) \log \pi(y) = Z \sum_{y \in Y} q(y) \log \pi(y) = Z \mathbb{E}_{y \sim q}[\log \pi(y)]  
 867$$

869 Since  $Z$  does not depend on  $\pi$  in the gradient computation (it is treated as a constant in the  $\bar{\pi}$  sense),  
 870 maximizing the original objective is equivalent to maximizing  $\mathbb{E}_{y \sim q}[\log \pi(y)]$ .  
 871

Finally, recall that the  $M$ -projection of a distribution  $q$  onto a set of distributions  $\Pi$  is given by  
 872

$$873 \min_{\pi \in \Pi} \text{KL}(q \parallel \pi) = \mathbb{E}_q[\log \frac{q}{\pi}] = \mathbb{E}_q[\log q] - \mathbb{E}_q[\log \pi]  
 874$$

875 since  $\mathbb{E}_q[\log q]$  does not depend on  $\pi$ , the maximizer of  $\mathbb{E}_{\bar{\pi}}[R \log \pi]$  over  $\Pi$  coincides with  
 876  $\arg \min_{\pi \in \Pi} \text{KL}(q \parallel \pi)$ . Thus, the policy gradient update corresponds to the  $M$ -projection of  $q$  onto  
 877 the policy class.  $\square$   
 878

879 **Theorem B.3** (RL with binary reward as an EM algorithm). *Let  $Y$  be a finite set and let  $\Pi \subseteq \Delta(Y)$   
 880 be a set of feasible policies. Let  $R : Y \rightarrow \{0, 1\}$  be a binary reward function and  $P^*$  the set of  
 881 all optimal policies  $P^* = \{q : \mathbb{E}_q[R] = 1\}$ . Then, solving the Single-step reinforcement learning  
 882 objective using policy gradients is equivalent to performing the following optimization procedure:*  
 883

$$884 q_t = \arg \min_{q \in P^*} \text{KL}(q \parallel \pi_t), \quad \pi_{t+1} = \arg \min_{\pi \in \Pi} \text{KL}(q_t \parallel \pi)  
 885$$

886 This procedure is also known as EM with information projection.  
 887

888 *Proof.* Sampling  $y \sim \pi$  and accepting iff  $R(y) = 1$  is exactly rejection sampling onto the event  
 889  $S = \{y \in Y : R(y) = 1\}$ . The resulting distribution is  $\pi(\cdot | S)$ . By Lemma A.1 with  $p \leftarrow \pi$ , this  
 890  $\pi(\cdot | S)$  solves

$$891 \min_q D_{\text{KL}}(q \parallel \pi) \quad \text{s.t.} \quad \mathbb{E}_q[R] = 1$$

892 establishing the I-projection. Applying Lemma A.2 on the RL objective gives us the M-projection.  
 893  $\square$   
 894

895 **Proposition B.4** (Convergence to minimum KL solution). *Under the setting appear in theorem  
 896 B.3 and assume  $\Pi$  is an e-flat (exponential-family) model with full support, the optimal set  $P^*$  is  
 897 nonempty and realizable (i.e.,  $\Pi \cap P^* \neq \emptyset$ ). Then:*

898 (1) *If the M-projection is exact at every step, then  $(\pi_t)$  converges to*

$$900 \pi^\dagger = \arg \min_{\pi \in P^* \cap \Pi} D_{\text{KL}}(\pi \parallel \pi_0)$$

901 (2) *If the M-projection is inexact but, for some errors  $\varepsilon_t \geq 0$ , it holds that*

$$902 D_{\text{KL}}(q_t \parallel \pi_{t+1}) \leq \min_{\pi \in \Pi} D_{\text{KL}}(q_t \parallel \pi) + \varepsilon_t \quad \text{with} \quad \sum_{t=0}^{\infty} \varepsilon_t < \infty$$

903 then  $\pi_t$  also converges to the same limit  $\pi^\dagger$ .  
 904

905 *Proof.* The I-step is always an exact I-projection (Lemma A.1). In the case of an exact M-step, the  
 906 iterative process is EM with information projections. The e-/m-flat geometry yields the Pythagorean  
 907 identities implying convergence to  $\pi^\dagger$  (Dempster et al., 1977; Csiszár, 1984; Amari & Nagaoka,  
 908 2000). When the M-step only ensures a (near-)minimization up to summable errors, the iteration is  
 909 GEM: monotone improvement and convergence follow from the GEM theory of Wu (1983) together  
 910 with generalized alternating minimization for Bregman divergences (Gunawardana et al., 2005),  
 911 which, under the same e-/m-flat assumptions, selects the same minimum-KL limit  $\pi^\dagger$ .  $\square$   
 912

918 **Practical considerations.** Our theoretical equivalence should be interpreted with the following  
 919 caveats:  
 920

921 • Beyond REINFORCE. In practice, many policy gradient algorithms such as GRPO and PPO re-  
 922 place the raw reward  $R(y)$  with an advantage estimate  $A(y)$ . Since this substitution is a control  
 923 variate technique, it leaves the expected gradient direction unchanged while reducing its variance.  
 924 Thus, our projection-based interpretation continues to hold.

925 • The optimal policy set  $P^*$  defined by the linear constraint  $\mathbb{E}_q[R] = 1$  is an  $m$ -flat family, but the  
 926 representable policy set  $\Pi$  induced by a neural network parametrization is not in general  $e$ -flat.  
 927 This may prevent exact convergence to the minimum-KL solution described above. Nevertheless,  
 928 our theorem provides a principled explanation for the bias observed in practical RL algorithms.

929 **B.2 KL REGULARIZATION**

930 We will start by analyzing the setting of RL with KL regularization:

931 **Theorem B.5** (The solution to RL with KL regularization). *Let  $\Delta$  be the set of probability measures  
 932 on  $\mathcal{Y}$ , and  $\Pi \subseteq \Delta$  a nonempty feasible policy class. Fix a base policy  $\pi_0 \in \Pi$  and a reward  
 933  $R : \mathcal{Y} \rightarrow \mathbb{R}$ . For  $\beta > 0$ , consider the penalized problem*

$$934 \max_{\pi \in \Pi} \mathbb{E}_\pi[R] - \beta \text{KL}(\pi \| \pi_0), \quad (1)$$

935 and let  $\pi_\beta^*$  be any maximizer with value  $\eta_\beta = \mathbb{E}_{\pi_\beta^*}[R]$ . Then  $\pi_\beta^*$  also solves the constrained problem

$$936 \min_{\pi \in \Pi} \text{KL}(\pi \| \pi_0) \quad \text{s.t.} \quad \mathbb{E}_\pi[R] = \eta_\beta. \quad (2)$$

937 Conversely, if  $\hat{\pi}$  solves equation 2 for some feasible target  $\eta$ , then there exists  $\beta > 0$  such that  $\hat{\pi}$   
 938 solves equation 1 and  $\mathbb{E}_{\hat{\pi}}[R] = \eta$ .

939 *Proof.* From Korbak et al. (2022) we know that if  $\Pi = \Delta$ , the solution to Equation 1 is the expo-  
 940 nentially tilted distribution

$$941 q_\beta(y) = \frac{\pi_0(y) e^{R(y)/\beta}}{Z_\beta} \quad Z_\beta := \int e^{R(y)/\beta} \pi_0(y)$$

942 For the more general case where  $\Pi \in \Delta$  whenever  $Z_\beta < \infty$ , we can write for any  $\pi \in \Pi$ :

$$943 \mathbb{E}_\pi[R] - \beta \text{KL}(\pi \| \pi_0) = \int R \pi - \beta \int \log\left(\frac{\pi}{\pi_0}\right) \pi \\ 944 = -\beta \int \log\left(\frac{\pi}{e^{R/\beta} \pi_0}\right) \pi \\ 945 = -\beta (\text{KL}(\pi \| q_\beta) - \log Z_\beta)$$

946 Hence maximizing equation 1 over  $\Pi$  is equivalent to

$$947 \pi_\beta^* = \min_{\pi \in \Pi} \text{KL}(\pi \| q_\beta).$$

948 By optimality, for every  $\pi \in \Pi$ ,

$$949 \text{KL}(\pi_\beta^* \| q_\beta) \leq \text{KL}(\pi \| q_\beta).$$

950 Using the decomposition  $\text{KL}(\pi \| q_\beta) = \text{KL}(\pi \| \pi_0) - \beta^{-1} \mathbb{E}_\pi[R] + \log Z_\beta$ , we obtain for all  $\pi \in \Pi$ :

$$951 \text{KL}(\pi_\beta^* \| \pi_0) - \frac{1}{\beta} \mathbb{E}_{\pi_\beta^*}[R] \leq \text{KL}(\pi \| \pi_0) - \frac{1}{\beta} \mathbb{E}_\pi[R].$$

952 Rearranging,

$$953 \text{KL}(\pi_\beta^* \| \pi_0) \leq \text{KL}(\pi \| \pi_0) - \frac{1}{\beta} (\mathbb{E}_\pi[R] - \eta_\beta) \quad \forall \pi \in \Pi$$

954 Now, fix any  $\pi \in \Pi$  such that  $\mathbb{E}_\pi[R] = \eta_\beta$ . Plugging this equality into the inequality above kills the  
 955 last term and yields

$$956 \text{KL}(\pi_\beta^* \| \pi_0) \leq \text{KL}(\pi \| \pi_0)$$

i.e., among all  $\pi \in \Pi$  with  $\mathbb{E}_\pi[R] = \eta_\beta$ ,  $\pi_\beta^*$  minimizes  $\text{KL}(\cdot \parallel \pi_0)$ . This proves that  $\pi_\beta^*$  solves equation 2.

Now for the other direction. Suppose  $\hat{\pi} \in \Pi$  solves equation 2 at some feasible  $\eta$ . Consider the Lagrangian:

$$\mathcal{L}_\lambda(\pi) = \text{KL}(\pi \parallel \pi_0) + \lambda(\eta - \mathbb{E}_\pi[R])$$

By the KKT conditions for the equality constraint, there exists  $\lambda^* > 0$  such that  $\hat{\pi}$  minimizes  $\mathcal{L}_{\lambda^*}$  over  $\Pi$ . Equivalently,  $\hat{\pi}$  maximizes  $\mathbb{E}_\pi[R] - \beta \text{KL}(\pi \parallel \pi_0)$  over  $\Pi$  with  $\beta = 1/\lambda^*$ , and necessarily  $\mathbb{E}_{\hat{\pi}}[R] = \eta$  holds at the maximizer. Thus  $\hat{\pi}$  solves equation 1.  $\square$

**Corollary B.6.** *Assume there exists  $\pi^* \in \Pi$  achieving the maximal attainable expected reward  $R_{\max} := \sup_{\pi \in \Pi} \mathbb{E}_\pi[R]$ . Let  $\Pi_{\text{opt}} := \{\pi \in \Pi : \mathbb{E}_\pi[R] = R_{\max}\}$ . Then there exists  $\beta > 0$  such that for every  $\beta \in (0, \bar{\beta}]$ , any maximizer  $\pi_\beta^*$  of equation 1 satisfies  $\mathbb{E}_{\pi_\beta^*}[R] = R_{\max}$  and*

$$\pi_\beta^* \in \arg \min_{\pi \in \Pi_{\text{opt}}} \text{KL}(\pi \parallel \pi_0).$$

In words: once the KL penalty is small enough that the optimal reward is still achievable, the KL-regularized objective selects the minimum-KL optimal policy.

Now we will move to analyzing the setting of SFT with KL regularization:

**Lemma B.7** (The solution to SFT with KL regularization). *Let  $\Delta$  be the set of probability measures on  $\mathcal{Y}$ , and  $\Pi \subseteq \Delta$  a nonempty feasible policy class. Fix a base policy  $\pi_0 \in \Pi$  and  $q$  as the distribution producing the annotations for the SFT training. For  $\beta > 0$ , consider the following objective:*

$$\min_{\pi \in \Delta(\mathcal{Y})} -\mathbb{E}_{y \sim q}[\log \pi(y)] + \beta \text{KL}(\pi \parallel \pi_0) \quad (3)$$

Assume  $\Pi = \Delta$ , then the unique minimizer  $\pi_\beta^*$  is given by

$$\pi_\beta^*(y) = \frac{q(y)}{\beta W\left(\frac{q(y)}{\beta A(\beta) \pi_0(y)}\right)} \quad (4)$$

where  $W$  is the principal branch of the Lambert  $W$  function and the scalar  $A(\beta) > 0$  is chosen to satisfy the normalization  $\sum_y \pi_\beta^*(y) = 1$ .

If  $q(y) = 0$  for some  $y \in \text{supp}(\pi_0)$ , the formula holds in the limit, yielding  $\pi_\beta^*(y) \rightarrow \pi_0(y)$ . If  $\pi_0(y) = 0$  and  $q(y) > 0$ , the objective value is  $+\infty$  and no finite minimizer exists.

*Proof.* Write the Lagrangian

$$\mathcal{L}(\pi, \lambda) = -\sum_y q(y) \log \pi(y) + \beta \sum_y \pi(y) \log \frac{\pi(y)}{\pi_0(y)} + \lambda \left( \sum_y \pi(y) - 1 \right).$$

Stationarity  $\partial \mathcal{L} / \partial \pi(y) = 0$  gives

$$-\frac{q(y)}{\pi(y)} + \beta \left( \log \frac{\pi(y)}{\pi_0(y)} + 1 \right) + \lambda = 0 \iff \log \frac{\pi(y)}{\pi_0(y)} = \frac{q(y)}{\beta \pi(y)} - \left( 1 + \frac{\lambda}{\beta} \right).$$

Let  $A := \exp(1 + \lambda/\beta) > 0$ . Then:

$$\pi(y) = \pi_0(y) A^{-1} \exp\left(\frac{q(y)}{\beta \pi(y)}\right) \rightarrow \pi(y) \exp\left(-\frac{q(y)}{\beta \pi(y)}\right) = \pi_0(y)/A$$

Setting  $u_y := \frac{q(y)}{\beta \pi(y)}$  yields  $u_y e^{u_y} = \frac{q(y)}{\beta A \pi_0(y)}$ , whence  $u_y = W\left(\frac{q(y)}{\beta A \pi_0(y)}\right)$  and thus equation 4.

The normalizer  $A(\beta)$  is uniquely determined by  $\sum_y \pi_\beta^*(y) = 1$ . Strict convexity of equation 3 on the simplex implies uniqueness.  $\square$

1026 **Theorem B.8** (SFT with KL reg. does not guarantee the minimum-KL optimal policy). *Let  $R : \mathcal{Y} \rightarrow \mathbb{R}$  be a reward and  $R_{\max} = \sup_y R(y)$ . Define the minimum-KL optimal policy as the solution of*

$$1029 \quad \min_{\pi \in \Pi} \text{KL}(\pi \| \pi_0) \quad \text{s.t.} \quad \mathbb{E}_{\pi}[R] = R_{\max}. \quad (5)$$

1030 *Let  $\pi_{\beta}^*$  denote the unique minimizer of equation 3 from Lemma B.7. Then, in general, there is no*  
 1031  *$\beta > 0$  such that  $\pi_{\beta}^*$  equals the minimum-KL optimal policy.*

1033 *Proof. (Counterexample).* Let  $\mathcal{Y} = \{1, 2, 3\}$ ,  $R(1) = R(2) = 1$ ,  $R(3) = 0$ . Take  $\pi_0 = (0.6, 0.2, 0.2)$ , hence  $\pi^{\min \text{KL}} = (0.75, 0.25, 0)$ . Let  $q = (0.5, 0.5, 0)$ , which is optimal ( $q(S) = 1$ ). We show that no  $\beta > 0$  yields  $\pi_{\beta}^* = \pi^{\min \text{KL}}$ .

1037 Using the stationary condition from the proof of Lemma B.7, and assume  $\pi_{\beta}^* = \pi^{\min \text{KL}}$ . We get  
 1038 this set of equations:

$$1039 \quad -\frac{0.5}{0.75} + \beta \left( \log \frac{0.75}{0.6} + 1 \right) + \lambda = 0, \quad -\frac{0.5}{0.25} + \beta \left( \log \frac{0.25}{0.2} + 1 \right) + \lambda = 0$$

1042 which has no solution, thus a contradiction.  $\square$

1043 *Counterexample.* Take  $\mathcal{Y} = \{1, 2, 3\}$  with  $R(1) = R(2) = 1$ ,  $R(3) = 0$ . Let  $\pi_0 = (0.6, 0.2, 0.2)$ ,  
 1044 then the minimum-KL optimal policy is  $\pi^{\min \text{KL}} = (0.75, 0.25, 0)$ . Choose an *optimal* annotator  
 1045  $q = (0.5, 0.5, 0)$ .

1046 Assume for contradiction that there exist  $\beta > 0$  and  $\lambda \in \mathbb{R}$  such that  $\pi_{\beta}^* = \pi^{\min \text{KL}}$ . The first-order  
 1047 condition from Lemma B.7 reads, for each  $y$ ,

$$1048 \quad -\frac{q(y)}{\pi(y)} + \beta \left( \log \frac{\pi(y)}{\pi_0(y)} + 1 \right) + \lambda = 0.$$

1049 Plugging  $\pi^{\min \text{KL}}(1) = 0.75$ ,  $\pi^{\min \text{KL}}(2) = 0.25$ ,  $\pi_0(1) = 0.6$ ,  $\pi_0(2) = 0.2$ ,  $q(1) = q(2) = 0.5$ ,  
 1050 we get

$$1051 \quad -\frac{0.5}{0.75} + \beta \left( \log \frac{0.75}{0.6} + 1 \right) + \lambda = 0,$$

$$1052 \quad -\frac{0.5}{0.25} + \beta \left( \log \frac{0.25}{0.2} + 1 \right) + \lambda = 0.$$

1053 Subtract the first equation from the second to eliminate  $\lambda$ . Using  $\log \frac{0.75}{0.6} = \log \frac{0.25}{0.2} = \log(1.25)$ ,  
 1054 the  $\beta$ -terms cancel and we obtain

$$1055 \quad -2 - \left( -\frac{2}{3} \right) = -\frac{4}{3} \neq 0,$$

1056 a contradiction. Hence no  $\beta > 0$  yields  $\pi_{\beta}^* = \pi^{\min \text{KL}}$  in this setting.  $\square$

## 1064 C TRAINING AND EVALUATION DETAILS

### 1065 C.1 LLM EXPERIMENTS

1066 Unless otherwise stated, all reinforcement learning experiments were conducted using GRPO (Shao  
 1067 et al., 2024).

1068 For the *Math* reasoning task, the training set provided final answers but lacked reasoning chains  
 1069 required for SFT training. To obtain these, we queried DeepSeek R1 (Guo et al., 2025a), sampling  
 1070 up to 16 responses per prompt and retaining a single response that matched the correct final answer.  
 1071 This yielded valid annotations for 96% of the dataset. For the *Science Q&A* task, we applied the  
 1072 same procedure with GPT-4o, obtaining correct annotations for the entire dataset.

1073 To construct the learning-forgetting trade-off curves (e.g., Figure 2), we followed the protocol be-  
 1074 low:

1075 1. Hyperparameter sweep. We trained multiple models under a broad sweep of hyperparame-  
 1076 ters (see Table 2).

1080 2. New-task evaluation. For *Math* and *Science Q&A*, accuracy was measured by comparing  
 1081 the model’s final answer to the ground truth, ignoring intermediate reasoning chains. For  
 1082 Tool Use, we extracted API calls from the output and matched them against ground-truth  
 1083 calls via regular expressions.  
 1084

1085 3. Previous-task evaluation. We assessed performance on unrelated benchmarks as described  
 1086 in Section 3.1, using the Language Model Evaluation Harness (Gao et al.,  
 1087 2024).  
 1088

1089 4. Pareto filtering. From the trained models, we retained only those lying within 2 accuracy  
 1090 points of the Pareto frontier.  
 1091

1092 5. Curve fitting. An exponential function was fit to the filtered points to produce the trade-off  
 1093 curves.  
 1094

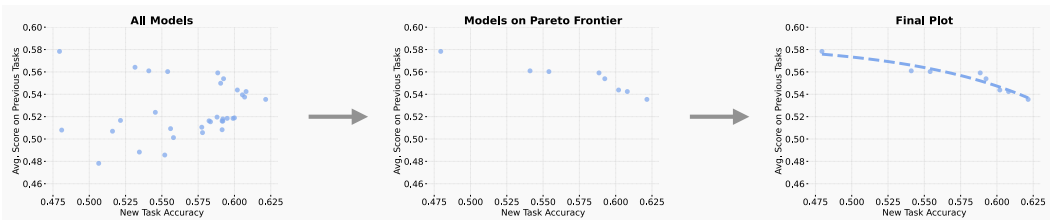


Figure 7: Example for the process of creating the pareto frontier plots

Hyperparameter	SFT / SIMPO	RL
Base Model	Qwen2.5 3B-Instruct	Qwen2.5 3B-Instruct
Learning Rate	{1e-5, 3e-5, 5e-5, 7e-5, 9e-5}	{1e-5, 2e-5, 3e-5, 4e-5, 5e-5}
Optimizer	adamw	adamw
LR Scheduler	{constant w. warmup, cosine w. warmup}	constant w. warmup
Warmup steps	50	50
Epochs	{1,2}	1
Batch Size	{16,32,64,128}	See Below
Max Grad Norm	1	1
bfloat16	True	True
Weight Decay	0	0
<i>GRPO-only hyperparameters</i>		
KL reg.		0
Group Size		64
Prompts per generation		8
num iterations ( $\mu$ )		{1,2}
Loss type		Dr. GRPO (Liu et al., 2025)

Table 2: Hyperparameters used for the LLM experiments. Curly braces {} indicate a sweep over the specified values. Additional parameters such as weight decay and max gradient norm were manually ablated; since they showed no significant effect on results, they were not included in the final sweep.]

## C.2 ROBOTIC EXPERIMENTS

We evaluated the RL-SFT forgetting gap in a robotic control setting using the OpenVLA-7B model (Kim et al., 2024) as our base policy in the SimplerEnv environment (Li et al., 2024b). The fine-tuning task was a pick-and-place scenario requiring the robot to grasp and lift a can, while forgetting was measured on a distinct manipulation task of drawer opening/closing. This setting complements our LLM results by probing whether the KL-forgetting relationship generalizes to embodied policies. To construct the pareto-frontier, we follow the same protocol as in the LLM experiments.

1134     **Data Collection.** Training data were collected by varying object placement over a  $10 \times 10$  grid of  
 1135     initial positions:  $\text{obj-init-x} \in [-0.35 - 0.12]$ ,  $\text{obj-init-y} \in [-0.02, 0.42]$ . For evaluation,  
 1136     we sampled 100 random object locations uniformly in this area.  
 1137

1138     **Supervised Fine-Tuning (SFT).** For each grid point, we collected 10 successful trajectories using  
 1139     the RT-1 (Brohan et al., 2022) model and filtered for successful trajectories. We trained models with  
 1140     batch sizes {16, 32, 64} and learning rates  $\{1 \times 10^{-6}, 3 \times 10^{-6}, 5 \times 10^{-6}, 7 \times 10^{-6}, 9 \times 10^{-6}, 1 \times 10^{-5}, 3 \times$   
 1141      $10^{-5}\}$ . Other hyperparameters were: AdamW optimizer, 1 training epoch, max gradient norm of 1,  
 1142     weight decay of 0, warmup of 10 steps, constant-with-warmup scheduler, and `bfloat16` precision.  
 1143

1144     **Reinforcement Learning (RL).** For RL, we trained using REINFORCE with an reward normaliza-  
 1145     tion baseline, without explicit KL regularization. At each iteration, 5 trajectories were collected  
 1146     per grid point. Rewards were binary success indicators of task completion. RL training used the  
 1147     same training config as SFT.

1148     C.3 MNIST EXPERIMENTS  
 1149

1150     All MNIST experiments were conducted using a 3-layer MLP with input dimension 785, hidden  
 1151     layers of sizes 512 and 256, and output dimension 10. The input consisted of a flattened  $28 \times 28$   
 1152     image concatenated with a binary indicator: +1 for ParityMNIST and -1 for FashionMNIST.  
 1153

1154     **Pretraining.** We pretrained the network jointly on ParityMNIST and FashionMNIST using small  
 1155     subsets of the original datasets (500 images from each). For ParityMNIST, the label was chosen  
 1156     uniformly at random among all digit labels with the correct parity.  
 1157

1158     **Fine-tuning methods.** In our experiments, we evaluated five fine-tuning strategies:  
 1159

- 1160     **1. GRPO.**
- 1161     **2. GRPO + KL regularization** with coefficient 0.1.
- 1162     **3. SFT 1:** all even digits mapped to label 0, all odd digits to label 1.
- 1163     **4. SFT 2:** even digits randomly mapped to  $\{0, 4\}$ , odd digits to  $\{1, 5\}$ .
- 1164     **5. SFT with oracle distribution:** annotations drawn from the minimum-KL distribution consistent  
 1165     with task correctness.

1166     **Oracle distribution.** Motivated by the KL-forgetting connection, we define the oracle distribution  
 1167     as the one that achieves perfect task accuracy while remaining closest (in KL divergence) to the  
 1168     pretraining distribution  $\pi_0$ . Concretely, for an input image  $x$  we compute  $\pi_0(\cdot|x) \in \mathbb{R}^{10}$  and the  
 1169     binary indicator vector  $R \in \{0, 1\}^{10}$  encoding which labels are correct given the digit’s parity. The  
 1170     oracle distribution  $q^*$  is the solution to:  
 1171

$$1172 \quad q^* = \arg \min_q D_{\text{KL}}(\pi_0 \| q) \quad \text{s.t.} \quad q^\top R = 1.$$

1173     Since KL is convex and the constraint is linear, we can calculate a closed-form solution for every  
 1174     image. We then sample from  $q^*$  to produce SFT annotations.  
 1175

1176     **Hyperparameter sweep.** For each method we trained models across a sweep of 15 learning rates  
 1177     logarithmically spaced between  $3e-6$  and  $1e-3$ , using either a constant-with-warmup or cosine-  
 1178     with-warmup scheduler, and training for 1 or 2 epochs. Including mid-training checkpoints, this  
 1179     produced approximately 500 runs per method.  
 1180

1181     C.4 CENTERED KERNEL ALIGNMENT  
 1182

1183     **Centered Kernel Alignment (CKA) (Kornblith et al., 2019)** Given representations  $X, Y \in \mathbb{R}^{n \times d}$ , define kernels  $K = XX^\top$ ,  $L = YY^\top$ . Let  $H = I - \frac{1}{n}\mathbf{1}\mathbf{1}^\top$  be the centering matrix.  
 1184     The centered kernels are  
 1185

$$1186 \quad \bar{K} = HKH, \quad \bar{L} = HLH.$$

1188 CKA is then computed as

$$1189 \quad \text{CKA}(K, L) = \frac{\langle \bar{K}, \bar{L} \rangle_F}{\|\bar{K}\|_F \|\bar{L}\|_F},$$

1190 where  $\langle A, B \rangle_F = \text{tr}(A^\top B)$ .

1191 **CKA with  $k$ -NN Alignment (CKNNA) (Huh et al., 2024)** Let  $\alpha(i, j) \in \{0, 1\}$  indicate whether  
1192  $i, j$  are mutual  $k$ -nearest neighbors in both  $X$  and  $Y$ . Define the masked inner product

$$1193 \quad \langle A, B \rangle_\alpha = \sum_{i=1}^n \sum_{j=1}^n \alpha(i, j) A_{ij} B_{ij}.$$

1194 CKNNA is then given by

$$1195 \quad \text{CKNNA}(K, L) = \frac{\langle \bar{K}, \bar{L} \rangle_\alpha}{\sqrt{\langle \bar{K}, \bar{K} \rangle_\alpha \langle \bar{L}, \bar{L} \rangle_\alpha}}.$$

1196 When  $\alpha(i, j) = 1$  for all  $i \neq j$ , CKNNA reduces to standard CKA.

## 1200 D ADDITIONAL RESULTS

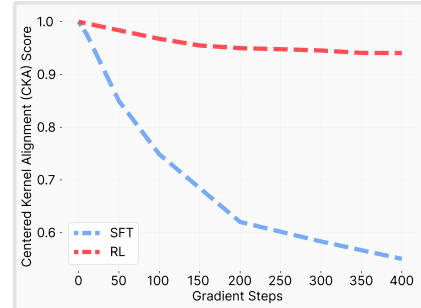
### 1201 D.1 REPRESENTATION PRESERVATION

1202 While benchmark accuracy provides an external measure of forgetting, it may conflate genuine loss  
1203 of capability with superficial effects such as formatting mismatch between tasks. To assess whether  
1204 fine-tuning alters the model more fundamentally, we analyzed changes to the model’s representa-  
1205 tions.

1206 **Experimental Setup.** To study how representations change between models, we compare their  
1207 embeddings on a shared dataset. Following prior work, we compare the relative geometry of the  
1208 embeddings—that is, how different inputs relate to each other. This geometry can be summarized  
1209 by a kernel (similarity) matrix, which encodes pairwise relationships among input embeddings.  
1210 Centered Kernel Alignment (CKA) (Kornblith et al., 2019) is a standard measure for comparing  
1211 such kernels, providing a way to quantify representational similarity between models.

1212 For this analysis, we constructed kernels from random  
1213 Wikipedia paragraphs, ensuring that the probe data are  
1214 unrelated to the fine-tuning tasks. We then compared the  
1215 kernels of the base model and its fine-tuned variants using  
1216 CKNNA (Huh et al., 2024), a local-neighborhood vari-  
1217 ant of CKA (see Appendix C.4 for details). Comparisons  
1218 were made between SFT and RL models that achieved  
1219 similar final accuracy on the new task, isolating rep-  
1220 resentational differences due to training method rather than  
1221 task performance.

1222 **Results.** Figure D.1 shows that RL-trained models re-  
1223 tain high representational similarity (CKNNA=0.94) to  
1224 the base model, with CKNNA scores remaining close  
1225 to one even after fine-tuning on the new task. In con-  
1226 trast, SFT-trained models exhibit substantial representa-  
1227 tional drift (CKNNA=0.56). These results indicate that  
1228 RL fine-tuning integrates new abilities while leaving the  
1229 overall representation space largely intact, whereas SFT  
1230 alters the geometry more extensively. Together with the  
1231 benchmark results, this suggests that RL is able to inte-  
1232 grate new abilities without disturbing the underlying rep-  
1233 resentational structure, while SFT incurs representational shifts that manifest as catastrophic forget-  
1234 ting.



1235 **Figure 8: CKA similarity to the base**  
1236 **model during training.** Although SFT  
1237 and RL achieve comparable task per-  
1238 formance, SFT models diverge substan-  
1239 tially in their representations, whereas  
1240 RL models remain more closely aligned  
1241 with the base model.

1242 D.2 SCALING AND FORGETTING  
1243

1244 Prior work has suggested that catastrophic forgetting diminishes as model size increases (Ramasesh  
1245 et al., 2021; Luo et al., 2023; Cossu et al., 2024). To evaluate this claim in our setting, we repeated  
1246 the SFT experiments from Section 3 using Qwen 2.5 models with 3B, 7B, and 14B parameters on  
1247 the Science Q&A task.

1248 The results, shown in Figure 9, demonstrate that although  
1249 larger models start with better general capabilities, the  
1250 trade-off between new-task performance and prior-task  
1251 retention remains unchanged: across all model sizes, SFT  
1252 improves new-task accuracy at the expense of forgetting.  
1253 In particular, to reach high accuracy on the Science Q&A  
1254 task, substantial degradation occurs in performance on  
1255 prior benchmarks regardless of model scale.

1256 D.3 OPTIMIZATION DYNAMICS  
1257

1258 To examine the link between parameter updates and  
1259 forgetting, we analyzed the optimization trajectory at the  
1260 level of individual training steps. For each update, we  
1261 computed two quantities:

1. **Forgetting direction.** Using the FashionMNIST eval-  
1264 uation set, we calculated the gradient of the loss with  
1265 respect to model parameters. We then measured the  
1266 cosine similarity between this gradient and the actual  
1267 parameter update from the training step. A positive  
1268 cosine indicates that the update increases FashionM-  
1269 NIST loss (catastrophic forgetting), while a negative cosine indicates an update that reduces it.
2. **KL shift.** We measured the change in KL divergence  
1271 between the model’s output distributions on the Par-  
1272 tyMNIST test set before and after the update.

1273 Plotting per-step KL change against the cosine similarity (Figure 11) revealed a strong correlation:  
1274 steps producing larger KL shifts tended to align more with the forgetting gradient. This analysis  
1275 demonstrates that at the level of optimization dynamics, catastrophic forgetting is driven by updates  
1276 that induce larger distributional shifts on the new task.

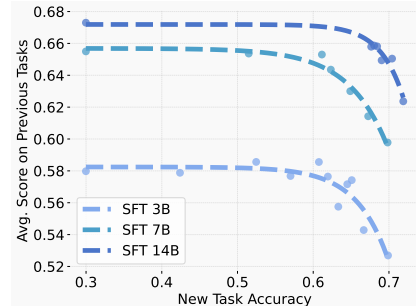
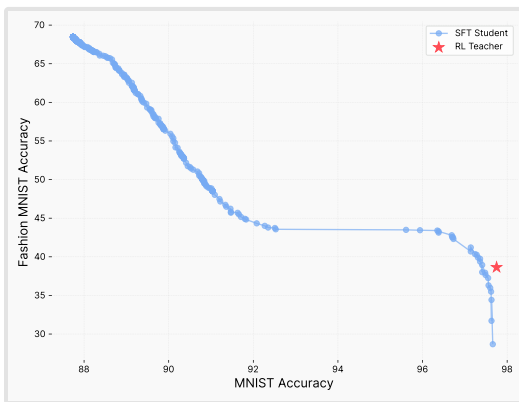


Figure 9: Pareto frontiers for SFT on Qwen 2.5 Instruct models of size 3B, 7B, and 14B on the Science Q&A task. All sizes exhibit the same fundamental trade-off—gains on the new task require forgetting prior capabilities.



1291 Figure 10: **SFT distillation from an RL teacher.** Accuracy trade-off between the new task  
1292 (MNIST) and the prior task (FashionMNIST). Sweeping student hyperparameters shows that SFT  
1293 can match the teacher within noise on both tasks. This suggests that what matters is not the opti-  
1294 mization path, but the distribution of the final model.

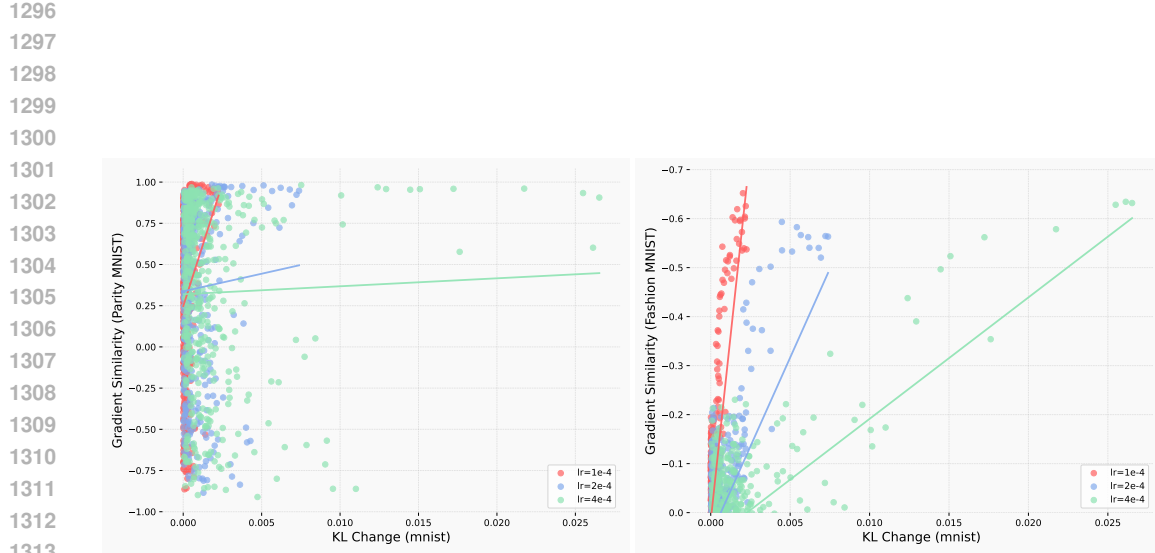


Figure 11: **Gradient similarity versus KL change.** (Left) On the new training task (ParityMNIST), gradient cosine similarity and KL change per step remain uncorrelated. (Right) On the prior task (FashionMNIST), the gradient similarity is more correlated with the KL change per step on the training task (ParityMNIST). Together, these plots show that taking a larger step on the current task induces gradients that are more similar in direction that forgets the most.

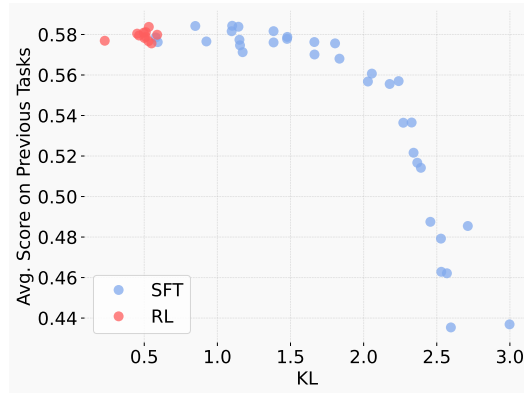


Figure 12: We plot the KL divergence between the base and fine-tuned model on the new task, alongside the corresponding forgetting performance across methods.